



Neural Mechanisms of Mechanosensation Within the Body

Citation

Williams, Erika. 2018. Neural Mechanisms of Mechanosensation Within the Body. Doctoral dissertation, Harvard Medical School.

Permanent link

<http://nrs.harvard.edu/urn-3:HUL.InstRepos:36923341>

Terms of Use

This article was downloaded from Harvard University's DASH repository, and is made available under the terms and conditions applicable to Other Posted Material, as set forth at <http://nrs.harvard.edu/urn-3:HUL.InstRepos:dash.current.terms-of-use#LAA>

Share Your Story

The Harvard community has made this article openly available.
Please share how this access benefits you. [Submit a story](#).

[Accessibility](#)

Neural mechanisms of mechanosensation within the body

Abstract

The ability to detect mechanical forces plays a critical role in organism behavior and physiology. One of the fundamental means by which we interact with our environment is through touch, which includes the ability to sense mechanical events such as pressure, impact, vibration, and changes in joint position. Similarly, one of the fundamental cues used by internal organ systems to regulate behavior and physiological responses is mechanical force within the body. Sensory systems in the intestinal tract detect stretch as these organs fill with and move food, playing a powerful role in the modulation of eating behavior. In addition, sensory systems also monitor the expansion and relaxation of the lungs during breathing to regulate respiration. Similarly, accurate monitoring of pressure within the vascular system plays a key role in regulation of cardiovascular function. Eating, breathing, and blood circulation constitute basic needs, yet our understanding of the sensory neurobiology in control of these functions is limited. To date, the molecular mechanosensors required remain unknown. However, the discovery of the mammalian mechanosensor Piezo2 raises the interesting possibility that this molecule is not only involved in detection of external mechanical cues in our skin, but may also sub-serve detection of mechanical cues within the internal organs of the body.

Table of Contents

Introduction	7
Mechanosensation in internal organs	7
The mammalian mechanosensor Piezo2.....	25
Recording mechanosensitive afferents in the vagus	30
Experiment 1: In Vivo imaging of Piezo-2 lineage neurons	35
Introduction	35
Methods.....	35
Results	35
Conclusions.....	39
Experiment 2: In vivo imaging of neurons that express Piezo2 in the adult.....	40
Introduction	40
Methods.....	40
Results	41
Conclusions.....	43
Experiment 3: Detection of stretch stimuli in Piezo2 knock-out ganglia.....	44
Introduction	44
Methods.....	44
Results	45
Conclusions.....	48
Summary	50
Bibliography.....	50

Glossary

AAV – adeno-associated virus

DRG – dorsal root ganglion

GLP1R – GLP1 receptor

GPR65 – G-protein coupled receptor 65

IGLE – intraganglionic laminar ending

IMA – intramuscular array

RAR – rapidly-adapting stretch receptor

SAR – slowly-adapting stretch receptor

siRNA – small interfering ribonucleic acid

Acknowledgements

Thank you to my family, the Liberles Lab past members and present, the Program in Neuroscience, MD PhD Program, and HST Program for the constant support and inspiration. Thank you to so many for technical help and expertise, and most notably the Harvard Animal Facilities; without you none of this work would be possible. Financial support for this work was through F30CA177170 and NIH MSTP-T32GM007754.

Introduction

Mechanosensation in internal organs

Internal organs are in constant motion, and similarly constantly subject to a variety of mechanical forces of critical physiological significance. Eating results in accumulation of food in the stomach and mechanical distension of the stomach wall. Neural detection of stomach stretch plays a critical role in feeding behavior. In addition, digestion involves the mechanical propulsion of food through sphincters and over approximately 25 feet of adult human intestine, a process similarly monitored and regulated by the nervous system. Breathing is characterized by the mechanical expansion and relaxation of the chest cavity to generate changes in pressure, and subsequent flow of air into and out of the lungs. Sensory neurons monitor respiratory movement to regulate breath frequency and depth, important variables for adequate oxygenation, carbon dioxide excretion, and protection of lung tissue. Lastly, the beating heart pumps blood and generates pulsatile flow and pressure within the vasculature. Neural monitoring of blood pressure initiates reflex regulation of heart rate and subsequent cardiovascular variables to preserve adequate tissue perfusion.

In this section, we will review mechanosensation in digestion, respiration, and circulation, with a focus on transmission of information from peripheral organs to the brainstem. Within each organ system, we will discuss physiologically relevant autonomic reflexes, neural response properties, and sensory neuron anatomy. One of the primary neural links from internal organs to the brain is the vagus nerve. Therefore, the vagus nerve will figure prominently in experiments and discussions, so a brief overview of its general anatomy and organization is provided.

The Vagus Nerve

The vagus nerve is one of the major body-to-brain neural connections, and mediates afferent sensory information transmission into the brain stem, as well as efferent motor command transmission out to target organs. Eighty percent of vagal fibers are sensory¹, and each sensory neuron extends one projection into the periphery to collect information from a target organ, and a second projection into the brainstem to transmit the information to central neural circuits. The sensory neuron cell bodies reside in ganglia, the nodose and jugular, located adjacent to the base of the skull. All sensory neurons use the neurotransmitter glutamate to communicate to central circuits. The remaining 20% of vagal fibers are motor fibers¹. The cell bodies of vagal motor neurons are located within nuclei in the brainstem, and send projections out from the brain to peripheral target organs. The neurotransmitter used by the motor neurons is acetylcholine. Therefore, the vagus nerve can be considered an anatomical highway shared by a sensory system carrying information centrally, and a motor system carrying commands peripherally. These two systems communicate closely; the sensory terminals in the brainstem are immediately adjacent to the nuclei containing the motor neuron cell bodies, and these neurons are known to make both direct and multi-neuron network connections to each other to provide reflex-like control of internal organ states²⁻⁴. For the purposes of a review on peripheral mechanosensation, we will focus on the response properties, anatomy, and physiological roles of vagal sensory neurons.

Gastrointestinal stretch

Physiology

Mechanical distension of the stomach plays a critical role in regulation of food intake. Not only does this intuitively coincide with nearly universal human experience following meals, but also careful experimentation over 60 years ago has elaborated on the physiological power and specific sensory cues relevant for regulation of meal consumption.

The earliest experiments to demonstrate the importance of gastrointestinal mechanosensation on feeding behavior were performed in dogs with surgically altered

upper gastrointestinal tracts ^{5,6}. Gastric fistulas allowed for artificial filling of the stomach, while esophagostomy allowed for artificial diversion of orally ingested food out of the esophagus and away from the stomach, dissociating oral ingestion and changes in stomach content. Filling the stomach via a fistula to a volume equivalent to approximately 40% of a normal meal size just prior to mealtime decreased oral consumption by an equivalent (30-50%) amount. The degree of intake inhibition was independent of the caloric value of the stomach filler; intake inhibition was the same if the stomach was filled with food, or calorically inert Karaya gum, suggesting the relevant sensory cue was the mechanical distension and not the chemical food content⁵. Intriguingly, if food was infused into the stomach at a time other than during eating, it had no impact on sham feeding, suggesting the temporal relationship between ingestion and stomach distension is critical for an effect⁶.

Conversely, when the food was diverted out of the esophagus and prevented from reaching the stomach, animals fed for longer. Furthermore, in diversion cases in which the stomach was distended either by replacement of food or by inflation of a rubber latex balloon, this effect was reversed and animals ingested less⁵. From these experiments, one can conclude: 1) Stomach distension is not necessary to terminate feeding because animals will stop feeding even if food does not reach the stomach. 2) Stomach distension does, however, play an important role in regulating the amount of food ingested because without stomach distension, animals eat more, and with it animals eat less. 3) The mechanical distension of the stomach, not the caloric content, is the relevant gastric cue for acute regulation of meal size, and this cue must occur at the same time as oral ingestion to impact acute feeding behavior.

Subsequent studies in rodents have confirmed these findings, and also delineated the effects of stomach-derived versus intestine-derived post-ingestion cues on eating behavior. In one elegant series of experiments ^{7,8}, rats were surgically implanted with a pyloric sphincter cuff and a gastric catheter. Inflation of the pyloric cuff prevented transit of stomach contents to the small intestine, while infusion through the gastric catheter allowed for experimenter-controlled delivery of gastric contents. These experiments demonstrated: 1) as in dogs, infusions in the stomach inhibited food intake independent of the caloric content of the infused solution, and 2) in contrast, caloric content did impact the degree of

feeding suppression when the pyloric cuff was left open and the contents could pass into the small intestine⁷. Both these findings are consistent with mechanically mediated inhibition of food intake by the stomach, and chemically mediated inhibition of food intake by the intestine.

The inhibition of food intake by gastric mechanosensation and intestinal chemosensation is thought to be dependent on intact vagal fibers. Animals consume larger meal sizes after surgeries in which vagal innervation of the stomach is disrupted, and infusion of volume into the stomach no longer suppresses food intake in vagotomized animals^{9,10}. Similarly, the suppression of meal size by chemical cues in the intestine is dependent on an intact vagus nerve^{11,12}, though it should be noted not all studies have found this effect^{13,14}. Despite the shortcomings of non-selective vagotomy experiments, these results suggest a key role for vagal afferents in regulation of feeding, and demonstrate a clear distinction between vagal gastric mechanosensors and intestinal chemoreceptors.

The experiments in animals are directly relevant to humans. Surgical methods to induce weight loss in people bear resemblance to experimental manipulations of stomach distension. A central goal of bariatric surgery is to reduce stomach capacity such that the same amount of food will cause greater distension. Reduction of gastric capacity can be achieved via several different surgical alternatives, including implantation of a volume-occupying balloon (gastric balloon), application of a constrictive band (banding), stapling of the stomach to reduce its effective volume (vertical banded gastroplasty), and stapling and resection most of the stomach pouch to leave a residual tube-like gastric sleeve (sleeve gastrectomy)¹⁵. Implantation of a balloon typically filled to a volume of 750-900 milliliters in the stomach of human patients has been shown to improve weight loss when compared to non-operative interventions^{16,17}. Similarly, banding and gastroplasty result in ~15% weight loss maintained over >10 years, whereas control subjects only lost ~2%; these results were accompanied by a decrease in long-term mortality likely secondary to the reduction in cardiovascular risk factors and diabetes associated with obesity¹⁸⁻²⁰. The most effective, 'gold-standard' weight loss surgery is the gastric bypass, in which only a very small residual stomach is connected to the distal small intestine to both reduce the stomach volume and the absorptive capabilities of the intestine²⁰, though sleeve gastrectomy alone

is nearly as effective in achieving weight loss¹⁵. In short, surgical reduction of the stomach volume is an effective weight loss tool in the face of the growing obesity epidemic, an effect likely mediated in large part through manipulation of vagal gastrointestinal mechanosensation.

Response properties

The impact of mechanical stomach distension on feeding prompted investigation of the operative sensory mechanisms. Only a few years following the initial canine physiology experiments described above, Paintal, Iggo, and colleagues described the first electrophysiological recordings of vagal afferents in response to distension of the stomach^{21,22}. In initial experiments, the cervical vagus trunk was serially sub-divided into fiber strands, and responses in each strand were recorded while a latex balloon was inflated in the stomach. Using this method, gastric stretch-responsive units could be isolated from units responsive to heart beats or the respiratory cycle, confirming the existence of a unique stomach stretch sensory neuron class. Furthermore, the endings of these fibers were thought to be likely located in the muscular stomach wall because their activity could be evoked by digital compression of the stomach, but not by stroking the mucosal or peritoneal gastric surfaces^{21,22}.

Gastric mechanoreceptors have consistent response properties. All fibers responded to distension quickly, exhibited firing rates of 25-60 impulses/second during the distension, and returned to baseline levels of activity immediately following relief of the distension. All but one of the fibers tested were either non-adapting or slowly adapting, with little change in the firing rate even during minute or multi-minute long distensions. Step-wise increases in the volume of distension generated a linear increase in the firing rate, though the threshold of distension required for fiber activation varied widely²¹. Furthermore, induction of muscular contractions of portions of the stomach wall in which the receptive ends of these fibers were found would elicit activity in the gastric receptors that was even more robust than that caused by passive distension²². Therefore, the relevant cue for fiber activation is not intra-gastric pressure per se, but the tension within the muscular wall of the stomach. Gastric stretch receptors are therefore considered 'in-

series' tension receptors, and monitor not only passive tension of the stomach wall but also active tension generated by muscular contraction in physiologically relevant ranges. A corollary to the observation that gastric mechanoreceptors are in-series is that the slow adaptation observed in tension receptor firing rates may at least in part reflect muscular relaxation of the stomach wall, and may not be an intrinsic property of the mechanoreceptor. The same properties were found for distension-sensitive vagal afferents that terminated in the esophagus or the small intestine²³. Similar properties have been subsequently described in gastric mechanoreceptors in multiple studies ²⁴⁻²⁷.

Subsequent studies sought to identify the molecular mechanism by which mechanical forces are transduced into a neural signal within vagal gastrointestinal mechanoreceptors. However, despite decades of recordings, it is unclear whether vagal afferents themselves are directly mechanosensitive, or whether they are transmitting information from mechanosensitive enteric neurons or non-neuronal gastrointestinal cells. Three arguments have been cited to support the idea that vagal afferents are directly mechanosensitive²⁸. First, the latency of response following specific and rapid mechanical deformation of the muscular wall of the esophagus is < 6 milliseconds, a delay has been cited as too rapid for a mechanism other than direct mechanosensation. However, the delay between firing of an upstream neuron and its chemically-coupled downstream target has been calculated at 2 milliseconds in the mammalian brain, suggesting 6 milliseconds is more than sufficient for synaptic transmission, and casting doubt on this claim²⁹. Second, extracellular calcium is considered a necessary component for vesicular transmitter release, and vagal afferent mechanosensitivity is preserved both when extracellular calcium is removed, and in the presence of the calcium-channel blocker Cd²⁺. However, calcium-dependent transmission is not the only means of cell-cell communication; gap junctions for example would allow for rapid and extracellular calcium independent signal transduction³⁰. Finally, pharmacologic inhibition of candidate neurotransmitter receptors (e.g. glutamate receptors, purinergic receptors) has no impact on vagal mechanosensation, evidence taken to exclude a role for these putative second-messengers, though of course this represents a drastically incomplete survey of potential cell-cell signaling mechanisms. In summary, these data are not conclusive, leaving much ambiguity about the true site or

sites of mechanosensation in the gastric distension sensory pathway. The molecular mechanosensor, unsurprisingly in this context, remains unknown.

Anatomy

Despite ambiguity about the mechanism of mechanotransduction, the morphology of distension-responsive vagal afferents in the gastrointestinal tract is known. Isolated esophageal and stomach preparations have allowed for localization of mechanically sensitive 'hot spots', and concurrent labeling of vagal fibers innervating those sites^{31,32}. Hot-spots in the esophagus and the stomach are enriched and localized around intraganglionic laminar endings (IGLEs), a vagal terminal type closely associated with myenteric neuron ganglia located between the circular and longitudinal muscle layers. Consistent with hot-spot studies, genetically labeled distension-sensitive afferents, marked by expression of the G-protein-coupled receptor GLP1R, form dense IGLE terminals throughout the gastrointestinal tract and terminate centrally within the medial nucleus of the solitary tract³³.

A small number of studies have examined the structure and locations of IGLEs in hopes of providing clues as to the sites of mechano-transduction. IGLEs were initially described using silver staining methods in the esophagus³⁴ as lamellated endings surrounding and entering the capsule of collections of enteric neuron cell bodies. Electron microscopy of vagal endings in these myenteric ganglia showed close approximation of mitochondria-rich IGLE terminals with the ganglion neuropil and cell bodies, but did not reveal a classic synaptic ultrastructure associated with these contacts³⁵. The close association between IGLEs and enteric ganglia could support both the idea that vagal neurons receive signals from primarily mechanosensitive enteric cells, or that enteric ganglia could provide critical support to primarily mechanosensitive vagal neurons.

IGLEs can be found in the esophagus, stomach and proximal small intestine, consistent with the vagal response properties identified in all these sites. The greatest density of IGLEs is located in the stomach, with decreasing density along the proximal intestinal length³⁶⁻³⁹. Some estimates suggest there are well over 1000 individual IGLE terminals in the stomach wall, and that though the density of innervation in the small

intestine is lower, the greater size of that organ would mean a larger absolute number of intestinal IGLEs than in the stomach³⁸. The high IGLE density in the stomach is consistent with the physiological importance of stomach stretch on feeding behavior. In addition, the high number of IGLEs in other sites suggests this terminal type also transduces important mechanical information from gastrointestinal sites outside the stomach.

IGLEs, notably, are not the only vagal terminal type in the muscular wall of the gastrointestinal tract. The second terminal type, named intra-muscular arrays (IMAs), are not nearly as widely distributed as IGLEs but rather seem to terminate around the gastro-esophageal junction, gastro-duodenal sphincter, and the junction between the proximal and middle segments of the colon³⁶. IMAs course between the longitudinal smooth muscle layers, forming long branching parallel tracts that form synapse-like contacts with intrinsically oscillatory, gastric contraction pace-making cells termed interstitial cells of Cajal⁴⁰. Given the anatomical association with ICCs and sphincters, IMA-forming neurons are also posited to be mechanosensors, but definitive evidence for their response properties and physiological role remains elusive.

Summary

Mechanical distension of the stomach regulates meal size during feeding. An intact vagus nerve is required for the detection of stomach distension and reduction of meal size. A select subset of vagal afferents responds to stomach stretch with slowly adapting increases in firing rate in response to both passive distension and muscular contraction. Distension sensitive vagal afferents form IGLE-type terminal endings in the esophagus, stomach and intestine muscle walls. However, key questions remain about the identity of the relevant mechanosensory molecular apparatus, the primary site of mechanosensation, and the contributions of non-IGLE stomach muscle-innervating vagal sensory afferents.

Lung stretch

Physiology

The physiological control of respiration has been linked to the vagus nerve since the inception of the respiratory physiology field. Early respiratory physiologists noted that electrical stimulation of the transected vagus nerve trunk could induce either expiratory or inspiratory effort⁴¹. However, results were mixed and the physiological relevance of these observations was not clarified until the work of Hering and Breuer in 1868, when the artificial manipulation of nerves was abandoned in favor of description of the physiological responses to inflation and deflation of the lungs⁴².

Breuer noted that when the lung was inflated, further inspiratory movements were inhibited, and expiration was promoted. Inspiratory inhibition occurred despite development of profound hypoxia and independently of the chemical composition of the gas used to inflate the lungs, suggesting the relevant cue was less likely chemical, and more likely mechanical. The degree of inspiratory inhibition was directly correlated to the degree of lung expansion. The reflex also seemed to be physiologically relevant because it could be observed both if the lung were artificially inflated beyond normal physiological volumes, and also if the trachea were simply occluded at the peak of natural inspiration. The relevant stimulus was thought to be the expansion of the lung itself for two reasons: 1) Expansion of collapsed lungs also blocked inspiratory effort, meaning the reflex was intact even when intra-thoracic pressures were abnormally low and chest wall movements could not contribute. 2) Introduction of elevated thoracic pressure through a tube in the side of the chest did not impact inspiratory effort as long as the state of expansion of the lungs was held constant, meaning the critical cue was the mechanical movement of the lung and not the external pressure to which the lung was subject. This reflex is classically referred to as the Hering-Breuer inspiratory reflex, and can be abolished by cutting both vagus nerve trunks in the neck⁴².

Subsequent physiological studies have revealed intriguing features of the Hering-Breuer reflex that complicate current understanding of its physiological role. First, a similar reflex was also initially described in which holding the lungs in exhalation would prevent further exhalation⁴²; a finding that sparked many decades of debate about whether

the same neural pathways could underlie both the inspiratory and expiratory reflexes^{43,44}. Second, a series of experiments were undertaken to investigate the relevance of the reflex in man, which revealed four intriguing findings: 1) inspiratory inhibition to lung inflation was observed in infants up until 3-4 days of life, during which time the reflex strength decreased and ultimately was lost⁴⁵. 2) The reflex could only be observed in adults under anesthesia or, in one subject, unconscious from a head injury⁴⁶, but not in sleeping adults⁴⁷. 3) Surgical instillation of a nerve-blocking agent to the vagus trunk could block the Hering-Breuer reflex in anesthetized patients⁴⁶. 4) In contrast, in awake subjects, nerve block injections around the ninth and tenth cranial nerves at the base of the skull resulted in no change in breathing, though the injections in these experiments caused profound hypertension (presumably secondary to baroreceptor blockade), and insensitivity to hypoxia (presumably secondary to chemoreceptor blockade)^{48,49}. These data together suggest that the strength of the Hering-Breuer reflex changes with development, and is influenced by subjects' state of consciousness. The questions raised about the role of the reflex in awake, normal humans remain unanswered.

Lung inflation induces other reflex effects beyond the Hering-Breuer inhibition of inspiration. Two other prominent reflex effects occur with lung inflation. First, physiological inspiration causes an increase in heart rate⁵⁰. However, careful experiments in which lung distension was isolated from changes in blood flow in the cardiopulmonary system and from chemical changes in the blood secondary to respiration suggested the relevant cue in this reflex is augmented cardiac venous return, to be discussed in subsequent sections⁵¹. Secondly, inspiration also triggers a reflex decrease of systemic vascular resistance⁵². In these experiments, expansion of the lungs by injecting physiologically relevant volumes of air resulted in a dose-dependent systemic vasodilation, while collapse of the lungs resulted in systemic vasoconstriction. Like in the Hering-Breuer reflex, the reduction in systemic vascular resistance was independent of the composition and temperature of the gas used to inflate the lungs. The effect was also maintained when the pressures in the carotid arteries and the aorta were held constant. Cutting pulmonary nerves and chemically inhibiting the sympathetic nervous system at the stellate ganglion in the neck could both abolish the reflex, suggesting it is mediated by communication between the vagus and sympathetic fibers. However, the same care in isolating pulmonary versus

cardiovascular contributions to this reflex was not taken as in other experiments, so specific conclusions cannot be drawn⁵³.

Response properties

As in the gastrointestinal stretch field, the description of the Hering-Breuer reflex drove the search for the operative neuronal elements, and their discovery only awaited the development of electrophysiology equipment and methods sensitive enough to record from single nerve fibers. Adrian was the first to identify individual pulmonary stretch-sensitive vagal afferents in 1933⁵⁴. The pulmonary mechanoreceptors Adrian identified generate large currents in fast-conducting A-fibers, explaining their identification over 10 years prior to their more elusive C-fiber mediated gastric mechanoreceptor counterparts. Work following this initial discovery identified two classes of mechanosensitive pulmonary afferents, distinguished by their adaptation rate and threshold of activation⁵⁵.

Slowly-adapting stretch receptors (SARs), defined as having a decline of firing rate of less than 55% within the first two seconds of a stretch stimulus, account for approximately 50% of all pulmonary inflation-sensitive vagal afferents⁵⁵. SARs are not only activated by experimental inflation, but also fire cyclically with the respiratory cycle, can be activated by forced lung deflation, and are also activated by contraction of smooth muscle surrounding the airways⁵⁶. Measurement of tracheal pressure thresholds of SAR activation suggests that at least half of all SARs are active during the resting respiratory cycle⁵⁷. Intriguingly, inhaled carbon dioxide inhibits SAR stretch sensitivity⁵⁸, an effect mediated within the lung because CO₂ inhibits SAR sensitivity without changes in arterial carbon dioxide levels^{59,60}. However, other than the inhibitory effect of CO₂, SARs are notably insensitive to other chemical stimuli⁶¹, and the oxygen content of the inhaled or infused gas does not impact the response properties of SARs⁵⁴. SARs therefore have a mechano-specific receptive field to rival their similarly slowly adapting gastric stretch sensitive cousins. These properties make SARs ideal candidates to mediate the Hering-Breuer inspiratory inhibition reflex.

In contrast, rapidly-adapting stretch receptors (RARs) are also activated by lung

inflation, but are defined as having firing rates that decrement by over 80% within the first two seconds of a stretch stimulus⁵⁵. RARs account for 40% of stretch-sensitive pulmonary afferents, though this varies with animal model investigated⁶². RARs exhibit a markedly higher threshold for activation compared to SARs; nearly no RARs are active during breathing at rest, though the majority would be activated at pressures exhibited during respiratory events such as coughing⁵⁷. In addition to these features, RARs are also sensitive to a number of irritating chemical mediators including pollutants such as ozone and wood smoke, a diversity of chemicals, pulmonary congestion, and introduction of hypo-osmotic solutions within the airways, earning them the name ‘irritant receptors’⁶³⁻⁶⁷. This mixed high-threshold mechanical and chemical receptive field suggests functional overlap with lung afferents that are purely chemo-sensitive without any mechanically sensitive response property component⁶¹. For these reasons, RARs are suspected to underlie reflex responses of hyperpnea and bronchoconstriction to offensive inhaled chemical agents. In addition, RARs can be sensitized, suggesting a role in reactive airway disease⁶³.

While SARs and RARs are considered broad categories of mechanosensitive lung afferents, detailed recordings reveal many fibers with properties intermediate between SARs and RARs that account for the remaining 10% of stretch-sensitive afferents per the SAR and RAR definitions provided above^{55,57,68}. Therefore, it may be more accurate to characterize fibers as belonging to a spectrum of adaptation and chemical sensitivity rather than to two fully discrete neuron groups. However, without a means to selectively and specifically manipulate RARs vs. SARs, the innervation patterns and physiological roles of each stretch-sensitive fiber type remains unclear.

Recent experiments have suggested the molecular identity of a lung mechanosensor⁶⁹, and these data will be presented in detail within the discussion of the discovery and elaboration of the mammalian mechanosensor Piezo2.

Anatomy

Vagal afferents travel along the major airways and provide terminals at all levels of the respiratory tree, from the trachea to the alveoli. The anatomical locations of SAR and

RAR terminals have been inferred from functional studies of terminal response properties, and their detailed terminal anatomy inferred based on the structures of vagal afferents found at these various anatomical sites.

SAR terminals are thought to be located in the smooth muscle surrounding airways⁶³. Three lines of evidence support this conclusion. First, SARs respond to direct mechanical probing of the airway smooth muscle, as well as to airway smooth muscle contraction^{56,70}. Second, SARs continue to function after the mucosa is stripped from isolated experimental preparations, but cease to function after disruption of the smooth muscle⁵⁶. Finally, SARs are not inhibited intra-airway anesthetics, supporting the conclusion that their terminals are isolated from the airway lumen⁵⁶. Myelinated vagal afferent terminals in pulmonary smooth muscle, inferred from the properties listed above to be SARs, have been characterized with both light and electron microscopy. As in other muscle mechanoreceptor endings, these terminals lose their myelin sheath close to their terminal site, and form close contacts with the basal lamina and connective tissue within the muscular layer^{71,72}. The distribution of SARs from the trachea to the alveoli seems to exhibit some species specificity, with anywhere from 40-90% being located in the intra-pulmonary airways versus in large extra-pulmonary sites⁷³.

RARs, in contrast, are thought to terminate in the submucosa and airway epithelium, a conclusion drawn from three pieces of evidence. First, light mucosal stroking inside the airway, as well as inhalation of chemical irritants, is able to elicit responses in RARs, while application of intra-airway local anesthetics such as lignocaine can suppress their activity^{57,63,74,75}. Second, the greatest area of RAR responsiveness is around the carina and large airway branch points, which is also the site of greatest intra-epithelial ending density⁵⁷. Finally, an intriguing and indirect observation is that animals that lack the cough reflex (e.g. mice, ferrets), also have very few intra-epithelial vagal terminals and RARs⁶². The sensitivity of RARs to intrapulmonary congestion, however, has also raised the possibility they are found close to lung vasculature as well⁷⁶. RARs are located in both large and small airways, and tend to have anatomically restricted receptive fields. For example, inflation of all airways and lung tissue distal to an RAR receptive site identified by gentle intra-airway

mucosal stroking fails to elicit activity of the RAR⁵⁷.

Intriguingly, genetically targeted labeling of vagal afferents that express the purinergic receptor P2RY1 selectively labels A-fibers that innervate neuroepithelial bodies in the epithelial lining of the lung, a terminal type that had been described previously but whose function has remained unknown^{77,78}. Activation of P2RY1 neurons results in apnea mirroring inhibition of inflation via the Hering-Breuer reflex, and in situ hybridization showed partial overlap between P2ry1 and the mechanosensor Piezo2, raising the possibility this neuron population is involved in the Hering-Breuer reflex and that Piezo2 could be the relevant mechanosensory molecule.

Summary

Mechanical distension of the lung regulates breathing depth and patterns. An intact vagus nerve is required for the detection of lung distension and changes in respiratory physiology. A select subset of vagal afferents responds to lung stretch. One subset is formed of slowly adapting, low-threshold, pure mechanosensors thought to terminate in the smooth muscle surrounding airways and mediate the Hering Breuer reflex. Others are rapidly adapting, high-threshold, mixed mechano- and chemo-receptors thought to terminate close to the airway epithelium and mediate cough and bronchoconstriction in response to irritants. However many conclusions within the field depend upon assumptions about structure-function relationships that still require rigorous examination, and ambiguity abounds concerning the molecular mechanisms, anatomy, and physiological relevance of lung mechanoreceptors.

Cardiovascular system

Physiology

The vagal reflex regulation of the cardiovascular system holds a fundamental place in the history of neuroscience. Otto Loewi and Henry Dale shared the Nobel Prize in

Physiology and Medicine in 1936 for the discovery of the first neurotransmitter, acetylcholine, released by the motor fibers of the vagus nerve to cause a decrease in heart rate⁷⁹. Just two years later, Corneille Heyman was awarded the same prize for the discovery that sensory nerves in the large vessels leaving the heart monitor pressure and blood chemistry to regulate the cardiopulmonary system, in a reflex arc through the vagal motor fibers investigated in Dale and Loewi's work. These critical experiments delineated the neural pathway of the baroreceptor reflex, in which increases in blood pressure cause a reflex decrease in heart rate on a beat-to-beat basis, allowing for maintenance of a constant blood pressure^{80,81}. The baroreceptor reflex is important both for prevention of hypertension, and of hypotension. Surgical removal of vagal afferents in the aortic arch and carotid bulb results in chronic hypertension⁸². In addition, without reflex accommodation of blood pressure, moving from a lying to a standing position would result in such a dramatic fall in cerebral perfusion that it would lead to loss of consciousness. Vaso-vagal syncope and orthostasis are, in fact, very common clinical complaints. Furthermore, decrements in the baroreceptor reflex with age and the concomitant inability to regulate blood pressure with changes in position is associated with increased falls, fractures, and mortality in people⁸³.

The baroreceptor reflex is not the only cardiopulmonary reflex mediated by vagal sensory fibers. Two other prominent reflexes are controlled by vagal afferents. The first, the Bainbridge reflex, serves to regulate intravascular volume status. Increased atrial volume results in two reflex effects: 1) an increase in heart rate to move the extra venous blood through the heart, and 2) an increase in urine output to reduce intravascular volume^{51,84}. Initially, inspiration was thought to drive the reflex increase in heart rate, as noted previously in the discussion of pulmonary reflex physiology. However, because the heart, lungs, and great vessels are all housed in the thorax, changes in intrathoracic pressure impacts the distribution of blood in all these organs. Reductions in intrathoracic pressure during inspiration augments the venous return of the blood to the heart, and careful isolation of this variable from inspiration itself revealed the cardiac chamber dilation to be the relevant cue^{51,84}.

The second reflex, termed the Bezold-Jarisch reflex, is thought to be a cardio-protective reflex in which both mechanical stretch and application of irritant chemical cues

to the muscular heart wall causes a reflex bradycardia, hypotension, coronary artery dilatation, and apnea^{85,86}. Reduction of heart rate reduces metabolic demand of cardiac tissue, systemic hypotension reduces the resistance against which cardiac myocytes need to pump blood, and coronary dilation augments perfusion of cardiac tissue. Therefore, though it is unclear the extent to which mechanical versus chemical cues drive this reflex, the result is reduced work and improved oxygenation of cardiac myocytes. How the Bezold-Jarisch reflex interacts with the other cardiopulmonary reflexes to maintain normal blood pressure and perfusion remains an area of uncertainty⁸⁷.

Response properties

As searches for the operative neuronal elements in lung stretch were under way, Adrian's contemporaries were similarly identifying the neuronal elements with changes in activity synchronized with the beating heart. Bronk and Stella in 1932 were the first to isolate single units in the carotid sinus nerve that fired cyclically with systole during heart beats, and changed their firing rates linearly with increases in blood pressure from 40mmHg to 120mmHg, the range of normal physiological blood pressures in the rabbit. They determined that increases in whole-nerve firing rates in response to increasing blood pressure was both a function of recruitment of more fibers, and increases in firing rate in individual fibers. Furthermore, the arterial baroreceptors they identified, as with several other vagal stretch-sensitive elements, are slowly-adapting⁸⁸. Subsequent studies have confirmed vagal sensory fibers are exquisitely tuned to pressure changes within the great vessels exiting the heart to deliver blood to the body and brain⁸⁹⁻⁹³. Intriguingly, despite their slow adaptation rate, vagal baroreceptors do shift their baseline and thresholds following prolonged exposure to hyper or hypo-tension, suggesting why this sensory apparatus would not be sufficient to counteract chronic hypertensive disease⁹³. The stress history of the vessel wall impacts baroreceptor responsiveness⁹².

Mechanosensitive afferents in the cardiovascular system are not only located in the major vessels, but also detect mechanical forces in the heart walls. Cardiac receptors can be further classified based on the period of the cardiac cycle during which their activity peaks. Some afferents are maximally active during atrial contraction, and exhibit increases in

firing rate with increases in heart rate, suggesting sensitivity to active changes in atrial wall stretch. Other receptors respond during atrial filling, and exhibit reduced activity with increases in heart rate. These receptors adapt slowly to changes in pressure, suggesting they act primarily as measures of overall wall strain. Both of these atria-sensitive fibers are exclusively fast-conducting A-fibers^{94,95}.

Ventricular fibers, in contrast, are much less common than atrial fibers (of cardiac mechanosensors, 75% are found in the atria and 25% in the ventricles) and can be classified further into two functionally distinct groups: one set responds primarily to ventricular contraction, and the other to gentle endocardial stroking^{96,97}. Most ventricular fibers are C-fibers, and also respond to intracardiac administration of a broad array of chemical compounds. The functional significance of this chemical sensitivity may relate to reflexes involved in response to cardiac stress or ischemia⁹⁸⁻¹⁰².

However, the specific molecular mechanisms used by cardiac mechanosensors remain undefined. Dissociated aortic baroreceptor neurons exhibit mechanically induced currents that can be blocked by gadolinium, suggesting the molecular mechanosensor may be a stretch-activated ion channel¹⁰³. In addition, both amiloride and its analogue, benzamil, inhibited pressure-evoked nerve activity in baroreceptor vagal afferents (Drummond, 2001), suggesting that the channel may bear relation to ENaC family mechanoreceptors. However, alternative possibilities abound, including evidence for example that knockout of Trpc5 attenuates the baroreceptor reflex¹⁰⁴. No candidate to date has yet been shown to fully abolish the reflex.

Anatomy

Vagal afferents innervate all four chambers of the heart, the aortic arch, and major branch arteries in the neck.

Endings within the cardiac chambers consist of three primary types, 1) complex un-encapsulated end-nets found most densely near junctions of the great veins entering the atria, and 2) anastomosing nets of fine neurites distributed throughout atrial and ventricular endocardium, some of which closely contact cardiac myocytes and 3) terminals surrounding “small intensely fluorescent” cells of unknown function in

cardiac ganglia^{94,105-108}. However, notably, within the cardiac chambers it seems that the same neuron can give rise to multiple of these ending types, complicating interpretations of structure-function relationships¹⁰⁷.

The neuronal endings in the great vessels have similarly been characterized into anatomical sub-types. Approximately 85% of vessel-terminating fibers directly innervate the vessel wall, forming “flower-spray” and “end-net” type terminals, while the remaining 15% terminate adjacent to other “small intensely-fluorescent” cells proximal and superficial to the wall itself¹⁰⁵. The most detailed architectural study of vagal afferents has been performed in the aortic arch, the site of most electrophysiologically active baroreceptors¹⁰⁸. Aortic nerve fibers in this region consist both of myelinated and unmyelinated fibers that pass through the vessel wall adventitia, coil and terminate within the vessel smooth muscle media layer. Within this layer, myelinated fibers lose their myelin sheath, and the axolemma is directly in contact with extracellular connective tissue. The tight approximation of neural elements with elastic elements of the wall speaks to a structure-function relationship well suited for transduction of mechanical forces and movement of the vessel wall.

Summary

Sensory monitoring of the mechanical movement of the heart and great vessels plays an important role in the regulation of heart rate and blood pressure. A select subset of vagal afferents responds to changes in pressure and strain during the cardiac cycle. Vagal baroreceptors, are thought to innervate the walls of large vessels, and drive reflex decreases in heart rate in the setting of hypertension, and reflex increases in the setting of hypotension. However, much ambiguity remains concerning the relative roles of heart versus vessel-terminating fibers, fibers of different conduction velocities, the interplay between chemical and mechanical stimuli, and of course the molecular mechanisms underlying detection of pressure and strain in this system.

Conclusions

The vagus nerve contains several afferent classes that monitor mechanical forces within the gastrointestinal, respiratory, and cardiovascular systems. Careful electrophysiological characterization and anatomical tracing has begun to elucidate some of the terminal types and putative physiological roles of these important sensory circuits. Genetic identification of the specific neurons involved has just begun to unfold. Vagal sensory neurons expressing GLP1R include the gastrointestinal mechanosensors³³. Vagal sensory neurons expressing P2RY1 are A-fibers and inhibit respiration, raising the possibility these are the slowly-adapting lung mechanoreceptors that underlie the Hering-Breuer reflex⁷⁷. However, to date, the identity of the receptor responsible for mechanotransduction itself in internal sensory systems remains unknown. Discovery of the molecular mechanisms at play could resolve debates about the site of primary mechanosensation, more clearly define the neuron populations involved, and also provide a pharmacological target for powerful manipulation of fundamental autonomic reflexes.

The mammalian mechanosensor Piezo2

Discovery

Extensive investigation into the molecular identity of mechanosensors has yielded discovery of several non-vertebrate mechanosensitive channel families, including the DEG/ENaC, TRP, TMCs and select K⁺ channels¹⁰⁹. The discovery of the Piezo family has offered intriguing molecularly specified mechanoreceptors for query in known mechanosensitive neural systems.

The members of the Piezo family, Piezo1 and Piezo2, were identified in a large-scale screening effort¹¹⁰. Cultures of intrinsically mechanosensitive mammalian cell lines were treated with siRNA designed to knock down expression of proteins of unknown function predicted to cross the cell membrane at least twice, a condition considered likely in a rapid mechanosensitive channel. The 71st candidate siRNA tested targeted Fam38a, now named Piezo1, and resulted in a several-fold reduction of the intrinsic mechano-sensitive current. Structural similarity led to identification of the closely related Piezo2. Overexpression of

these proteins in heterologous systems conferred mechanosensitivity to otherwise mechanically insensitive cells. Furthermore, immunohistochemistry revealed Piezo1 to be localized to the cell membrane, the physical site of mechanotransduction. Piezo2 was found by *in situ* hybridization to be expressed in a subset of dorsal root ganglion neurons, and knockdown of Piezo2 in DRG cultures resulted in a reduction of cells with rapidly inactivating mechanosensitive currents, providing strong evidence that Piezo2 plays a role in mechanotransduction in known mammalian mechanosensitive neurons. Notably, slowly inactivating mechanosensitive DRG neurons remained unperturbed by knockdown of Piezo2, suggesting additional mammalian mechanoreceptors remain to be discovered.

Subsequent work provided further evidence that Piezo1 and Piezo2 were in fact the molecular mechanosensitive element¹¹¹. Expression of Piezo proteins alone in lipid bilayers was sufficient to confer mechanosensitivity. Furthermore, recordings from membranes containing PIEZO proteins show single-channel currents activated by mechanical force that could be inhibited with ruthenium red, a non-selective cation channel blocker. Photo-bleaching experiments suggested that PIEZO forms tetramers within the cell membrane. These data together suggest that Piezo1 and Piezo2 assemble into pore-forming, cation channels capable of mechanotransduction independent of any other molecular elements.

In vivo properties

Invertebrate mechanosensation

Following their discovery and molecular characterization, subsequent work sought to elucidate the *in vivo* expression patterns and physiological relevance of Piezo1 and Piezo2. The first study to demonstrate the *in vivo* relevance of Piezo mechanosensors was not in mammals, but rather in the fruit fly *Drosophila melanogaster*¹¹². The Piezo family has one member that is expressed in *Drosophila*, *Dmpiezo*. Expression of a fluorescent reporter under the control of *Dmpiezo* resulted in fluorescence in a variety of sensory neurons, suggesting the possibility of a role in mechanosensation. *Dmpiezo* knockout flies, however, did not exhibit deficits in coordination, nor in the bristle mechanoreceptor potential,

suggesting Dmpiezo is not a key mechanoreceptor in adult flies. In contrast however, Dmpiezo knockout larvae exhibited reduced sensitivity to noxious mechanical stimuli. Isolation and recoding of *ppk* neurons, known to be specifically implicated in larval noxious mechanical sensitivity, demonstrated that Dmpiezo knockout causes complete loss of mechanosensitive currents in this neuron class. Therefore Dmpiezo plays a role in noxious mechanosensation in larvae, making it one of the first ion channels to have demonstrated both *in vitro* mechanosensitivity and a role in behavior *in vivo*.

Vertebrate dorsal root ganglia and skin sensation

With the development of mouse genetic tools, several studies have shown that Piezo2 plays a key role in multiple mechanosensory modalities in mammals^{113,114}. The Piezo2 protein can be found on sensory neuron terminals within the skin. Piezo2 can also be found within Golgi tendon organs and muscle spindle fibers, suggesting an additional role in sensation of joint and limb position. Concordant with these anatomical results, mice lacking Piezo2 show deficits in detection of vibration, light touch, hair deformation, low-force mechanical stimuli, and proprioception, without deficits in response to pain or temperature. In addition, Piezo2 expression is not limited to neurons; intriguingly, Piezo2 is also expressed in Merkel cells, a specialized cell type associated with mechanosensitive neuron terminals. Merkel cell -specific knockout of Piezo2 abolished the mechanosensitivity of Merkel cells, and resulted in a reduction in mechanosensitive currents and behavioral responses to low-force mechanical stimuli¹¹⁵. Therefore, it is likely that Piezo2 acts both in neurons and in Merkel cells to mediate low-force mechanosensation.

Vertebrate lung inflation and the Hering Breuer reflex

In addition to a role in external sensation of the skin and extremities, Piezo2 has also been implicated in mechanosensation in the respiratory system⁶⁹. Constitutive, global deletion of Piezo2 is lethal; knockout pups are cyanotic, with low arterial oxygen saturation, abnormal respiratory rhythms, and small airspaces on histological examination

of the lung, resulting in death within 24 hours of birth. To try to understand the relevant site of Piezo2 expression for this lethal phenotype, different mouse driver lines were used to selectively knock-out Piezo2 in the endothelium of blood vessels, neural crest derivative tissues such as the neuroepithelial bodies in the lung and sensory neurons within jugular ganglia, the trigeminal ganglia and of course the dorsal root ganglia, and in cranial placode-derived tissues such as the nodose ganglion. Piezo2 knockout specifically in the endothelium or in the nodose ganglion did not impact pup survival. However, Piezo2 knockout in the jugular ganglion, dorsal root ganglion, and trigeminal ganglion recapitulated the phenotype observed with global Piezo2 deletion. These data together suggest that Piezo2 expression in neural crest -derived tissues is necessary for survival, and that Piezo2 loss from the neural crest results in abnormal pup respiratory dynamics.

These observations beg the question of the role Piezo2 plays in the respiratory system in the adult animal. Optogenetic activation of neurons within the nodose-jugular complex that either currently express or have expressed Piezo2 during development results in apnea in the adult, implicating this neuron population in adult respiratory control. Conditional deletion of Piezo2 in the adult mouse nodose, jugular, and dorsal root ganglia results in a reduction of vagus nerve activity in response to inflation of the lung, a finding consistent with the role of Piezo2 in mechanosensation either within the neural crest or placode-derived tissues of this structure.

While deletion of Piezo2 from the placode-derived nodose sensory neurons is not lethal, these animals do exhibit abnormal respiratory cycles as adults. Furthermore, vagal responses to lung stretch are completely ablated in Piezo2 deletion in the nodose ganglion. This result raises interesting questions because it suggests that in the adult mouse, all vagal lung mechanoreceptors are in the nodose ganglion, and none in the neural crest -derived jugular ganglion. However, in pups loss of Piezo2 in the neural crest but not the nodose is lethal. Does this mean that the role of Piezo2 in the neural crest required for survival is not related to adult detection of lung inflation? How do the sensory roles of jugular versus nodose versus extra-vagal neurons evolve over the course of development? If detection of lung inflation depends on nodose Piezo2 expression, and loss of detection of lung inflation is non-lethal, what is the physiological significance of adult lung inflation monitoring? Where else is Piezo2 deleted in by the driver used in nodose ganglion deletion experiments,

and does this result in abnormalities that could explain the loss of lung stretch sensitivity in the adult? The dissociation of the role of Piezo2 in neural crest –derived versus cranial placode -derived tissues suggests it sub-serves more than one function in the respiratory system.

Role of Piezo2 in human mechanosensation

Piezo2 plays an important role in human mechanosensation and development. Gain-of-function mutations in Piezo2 have been shown to underlie a rare autosomal dominant form of distal arthrogryposis characterized by multiple distal contractures, ophthalmoplegia, ptosis, and restrictive lung disease¹¹⁶. Two families were identified with similar features; in one a Piezo2 point mutation resulted in faster recovery from inactivation, and in the other a Piezo2 missense mutation caused both faster recovery from inactivation and slower inactivation kinetics, both mutations that would translate to increased sensitivity to mechanical forces. Patients survive till adulthood and are fertile, but have characteristic facies with deep-set eyes, and difficulty with muscle movement including of the eye, back, neck, and both large and small joints of the extremities.

In contrast, two patients of different ancestry have been identified with complete Piezo2 loss-of-function mutations¹¹⁷. The Piezo2 variants found in these patients either had Piezo2 alleles with premature stop codons, or one allele with a premature stop codon and another with a missense mutation. These variants were unable to generate mechanosensitive currents when expressed in heterologous cell systems.

The two patients with these mutations both presented with a similar constellation of characteristics. Developmental features included congenital hip dysplasia, finger contractures, foot deformities, severe progressive scoliosis, hypotonia, delayed walking and head control, and a history of shallow breathing during infancy. As adults, both demonstrated a profound sensory ataxia, resulting in difficulty performing reaching tasks and an inability to walk or stand with eyes closed, consistent with deficits in proprioception. They were also unable to feel a vibrating tuning fork, had severely reduced light touch sensitivity, and exhibited chance performance of two-point discrimination on

glabrous skin. Temperature and pain sensitivity was normal. They also had intact light touch sensation on areas of hairy skin, suggesting a Piezo2-independent light touch sensory modality associated with hair. In summary, these patients exhibit similar sensory deficits as mice that lack Piezo2 as adults. However, importantly, human loss-of-function of Piezo2 is not necessarily lethal. Further characterization of the medical history during infancy and characterization of the respiratory system of these patients would be of great interest.

Conclusions

Piezo2 is a mammalian mechanosensor with demonstrated importance in detection of external mechanical cues. The molecular identities of the mechanosensors involved in detection of internal cues remain unknown, though the phenotypes of Piezo2 mutant mice and humans both suggest that Piezo2 could be involved in critical internal physiological reflexes. Therefore, we sought to determine if the neurons that have expressed or currently express Piezo2 in the nodose ganglion mediate detection of internal stretch, and whether Piezo2 knockout could alter neuron response properties.

Recording mechanosensitive afferents in the vagus

Introduction

Several experimental goals must be met to evaluate the role of Piezo2 in mammalian internal mechanosensation. A method to record the activity of vagal afferents of known molecular identity is required. Ideally, such an experimental design would allow for simultaneous recordings from multiple neurons within the same animal. Similarly, stimulus delivery paradigms must enable robust and consistent activation of mechanosensitive vagal afferents. These goals were achieved using in vivo calcium imaging with the well-known genetically encoded calcium indicator GCaMP3 in the nodose ganglion. These methods and results are elaborated elsewhere³³. However, for the purposes of understanding the experiments herein, a brief summary is provided below.

Methods

Transgenic mice used for imaging experiments were generated to provide ganglion-wide expression of the genetically encoded calcium indicator GCaMP3, either through use of a Vglut2-ires-Cre allele to drive Cre-dependent Gcamp3 expression in all vagal sensory neurons, or using a mouse line in which Gcamp3 is constitutively expressed in all cells in the mouse from birth. The nodose/jugular/petrosal ganglion complex was surgically exposed. The connections to the brainstem were transected, and connections to the periphery preserved. Imaging was performed with a Leica confocal microscope, and the confocal pinhole was reduced to avoid overlapping cells in the z-plane. Laser power did not exceed 90uW to prevent bleaching and tissue damage. Image analysis was performed first using Fiji; videos were aligned such that the same neurons were in the same location throughout all imaging experiments, neuron ROIs were manually selected, the average intensity within each ROI calculated for each frame, and these values were exported. Matlab was used to convert raw intensities into a $\Delta F/F$, where $\Delta F/F = (\text{intensity} - \text{average baseline intensity}) / \text{average baseline intensity}$.

Recording of neuron activity of known molecular identity was achieved by crossing mouse lines that express Cre recombinase in a subset of nodose ganglion cells, a Cre-dependent tdTomato reporter, and the constitutive GCaMP3 allele. Because all cells express GCaMP3, and targeted neurons were visualized by tdTomato expression, this enables a direct comparison of responses in Cre-positive and Cre-negative neurons. In triple cross animals, the wavelength range collected for GCaMP3 imaging was restricted to prevent bleed-through from the tdTomato channel. This resulted in baseline GCaMP3 fluorescence intensity measurements that were similar between tdTomato-positive and tdTomato-negative neurons (see dissertation thesis). In my PhD dissertation work, this allowed for evaluation of the response properties of nodose neuron subsets defined by expression of the markers Gpr65, Glp1r, P2ry1, Npy2r, and Mc4r.

Gastric distension was achieved by either of two methods: 1) inflation of a surgically implanted latex balloon affixed to a small rodent feeding needle and syringe, or 2) inflation of the stomach with nitrogen gas (flow rate 3-6 mL/min, 7-15 sec of inflation). Mice were fasted overnight for gastrointestinal experiments. Respiratory stimuli were delivered via

tracheal cannula connected to gas tanks that would deliver a fixed gas flow rate.

Gross blood pressure manipulations were attempted by rapidly injecting 1-3mL of lactated ringers into the mouse vascular supply via femoral vein catheter (4 mice). However, this stimulus failed to elicit any responses in the mice tested, and was abandoned.

Neurons were coded as responsive to gastrointestinal mechanical stimuli if either of two criteria were met: 1) maximal GCaMP3 fluorescence was > seven standard deviations above the baseline mean during the stimulus, or 2) if mean GCaMP3 fluorescence was > three standard deviations above baseline mean during the entire stimulus. Neurons were categorized as responsive to introduction of gases in the lung if they exhibited increases in fluorescence intensity during the stimulus at least three standard deviations or greater above a 30-second baseline mean intensity.

Results

The details of the results provided are discussed in detail in the dissertation defense, and in publication³³. Briefly, however, in vivo calcium imaging allows for the identification and characterization of sensory neuron populations in the vagus nerve in the living mouse. Stomach stretch causes a volume-dependent recruitment of approximately 17% of all electrically responsive vagal sensory neurons (Figure 1A). Lung inflation similarly recruited in a flow-dependent manner approximately 4% of vagal sensory neurons, many of which also showed increases in activity with the resting mouse respiratory cycle (Figure 1B,C). These mechanically responsive neuron subsets were activated independent of the chemical composition of the stimulus used (Figure 1D). In the case of stomach stretch, the same neurons were activated by distension with liquid diet or nitrogen gas inflation. In the case of lung stretch, the same neurons were activated by inflation with nitrogen, oxygen, or room air. These mechanically responsive subsets were unique from each other, and from the neuron population responsive to chemical stimuli applied in the small intestine (Figure 1E).

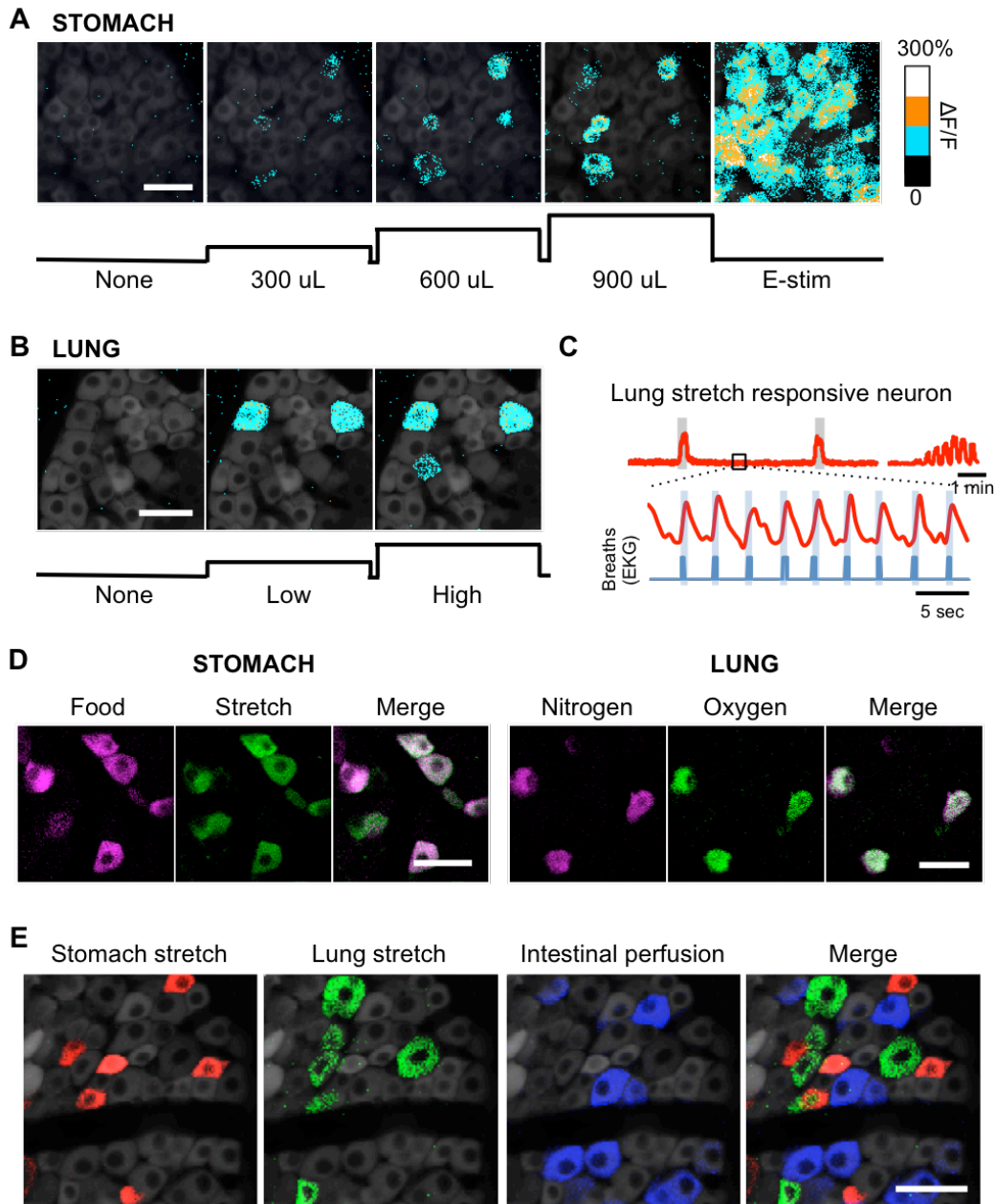


Figure 1. *In vivo* calcium imaging of vagal sensory neurons. (A) Increasing volumes of stomach distension (300, 600 and 900 μ L) cause volume-dependent recruitment of a vagal sensory neuron subset as measured by *in vivo* GCaMP3 fluorescence intensity. (B) Increasing flow rate of gases into the lung (low 0.5 L/min, high 1L/min) cause dependent recruitment of a vagal sensory neuron subset, as measured by *in vivo* GCaMP3 fluorescence. (C) Many of the lung stretch sensitive vagal afferents show cyclical changes in fluorescence intensity entrained to the resting respiratory cycle. (D) The recruitment of stomach and lung-stretch sensitive neurons is independent of the chemical identity of the stimulus used in organ stretch. (E) Representative images of GCaMP3 fluorescence signal in a vagal ganglion following tandem application of stomach stretch (red), intestinal glucose (blue), and lung inflation (green). All scale bars, 50 μ m. Modified from Williams, et al 2016.

Finally, using the triple transgenic strategy to label specific neuron subsets with the fluorescent protein tdTomato allowed for the identification of the response properties of these neuron populations. Neurons marked by expression of Cre under the control of *Glp1r*, or *GLP1R* neurons, accounted for most (85%) of the stomach stretch responsive cells (Figure 2A). In contrast, neurons marked by expression of Cre under the control of *Gpr65* accounted for most (66%) of the intestinally chemosensitive neuron subset (Figure 2B).

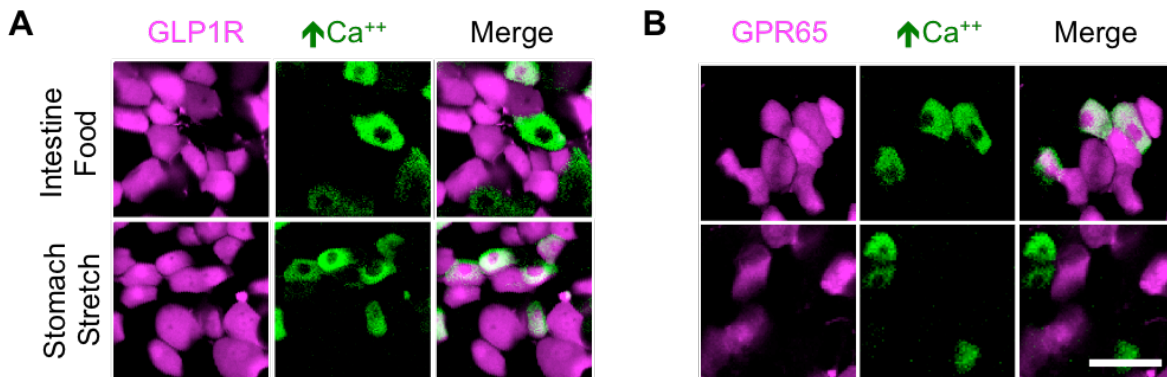


Figure 2. *In vivo* calcium imaging of molecularly defined vagal sensory neuron subsets. (A) Representative images of *GLP1R* neurons and increases in fluorescence of the calcium indicator *GCaMP3* in response to food in the intestine, and to stomach stretch. The stomach stretch, but not the intestinal food responsive neurons are completely contained within the *GLP1R* neuron subset. (B) Conversely, all of the intestine food responsive neurons are contained within the *GPR65* neuron subset. Scale bar, 50 μm . Modified from Williams et al, 2016.

Conclusions

The development of *in vivo* calcium imaging in the nodose ganglion allows for identification of gastric and lung mechanosensitive neuron populations, and concurrent identification of molecularly defined neuron subtypes. Therefore, *in vivo* imaging provides an excellent experimental platform to investigate the response properties of *Piezo2*-marked vagal sensory afferents.

Experiment 1: In Vivo imaging of Piezo2 lineage neurons

Introduction

If Piezo2 is the mechanosensor for internal mechanical stimuli, mechanosensitive vagal afferents should express Piezo2. To test this hypothesis, we used in vivo calcium imaging to examine the response properties of neurons that expressed a Cre-dependent tdTomato reporter in Piezo2-Cre mice.

Furthermore, the observation that selective activation of P2RY1 neurons causes apnea raises the possibility that P2RY1 neurons may also play a role in detection of lung stretch. In situ hybridization has shown partial overlap between neurons that express *P2ry1* and *Piezo2*⁷⁷, further suggesting that perhaps the relevant lung-stretch sensitive population consists of the neurons that express both *P2ry1* and *Piezo2*. Therefore, we also sought to examine the mechanical sensitivity of the P2RY1 neuron subsets.

Methods

We generated the triple knock-in mouse line *Piezo2-ires-Cre; lox-tdTomato; Rosa26-GCaMP3* (*Piezo2-GCaMP3**), and *P2ry1-ires-Cre; lox-tdTomato; Rosa26-GCaMP3* (*P2ry1-GCaMP3**), which allow for an in vivo nodose ganglion imaging approach involving constitutive expression of the genetically encoded calcium indicator GCaMP3, and the Piezo2-Cre-dependent expression of tdTomato. Imaging, stimulus administration, and analysis were performed as described previously.

Results

*Piezo2-GCaMP3** mice demonstrated expression of tdTomato broadly in satellite glial cells surrounding nodose ganglion neurons, and also within a subset of sensory neurons. Of 283 electrically responsive neurons (n = 3 mice), 98 (34.6%) expressed

tdTomato. P2ry1-GCaMP3* mice also demonstrated expression of tdTomato broadly in satellite glial cells surrounding nodose ganglion neurons, and in a subset of neurons as well. Of 211 electrically responsive neurons (n = 3 mice), 31 (14.7%) expressed tdTomato.

In PIEZO2 experiments, seventeen neurons were identified as responsive to lung stretch stimuli, a proportion of the total ganglion (7.2%) consistent with prior estimates of the size of the lung-stretch responsive population. Of these 17 lung stretch responsive neurons, 16 were positive for tdTomato (94%). Conversely, 16 of 84 (19%) tdTomato-positive neurons were responsive to lung stretch. From these data we conclude that nearly all lung-stretch responsive neurons have expressed Piezo2, and that lung-stretch responsive neurons account for approximately one-fifth of neurons that have expressed Piezo2 (Figure 3A).

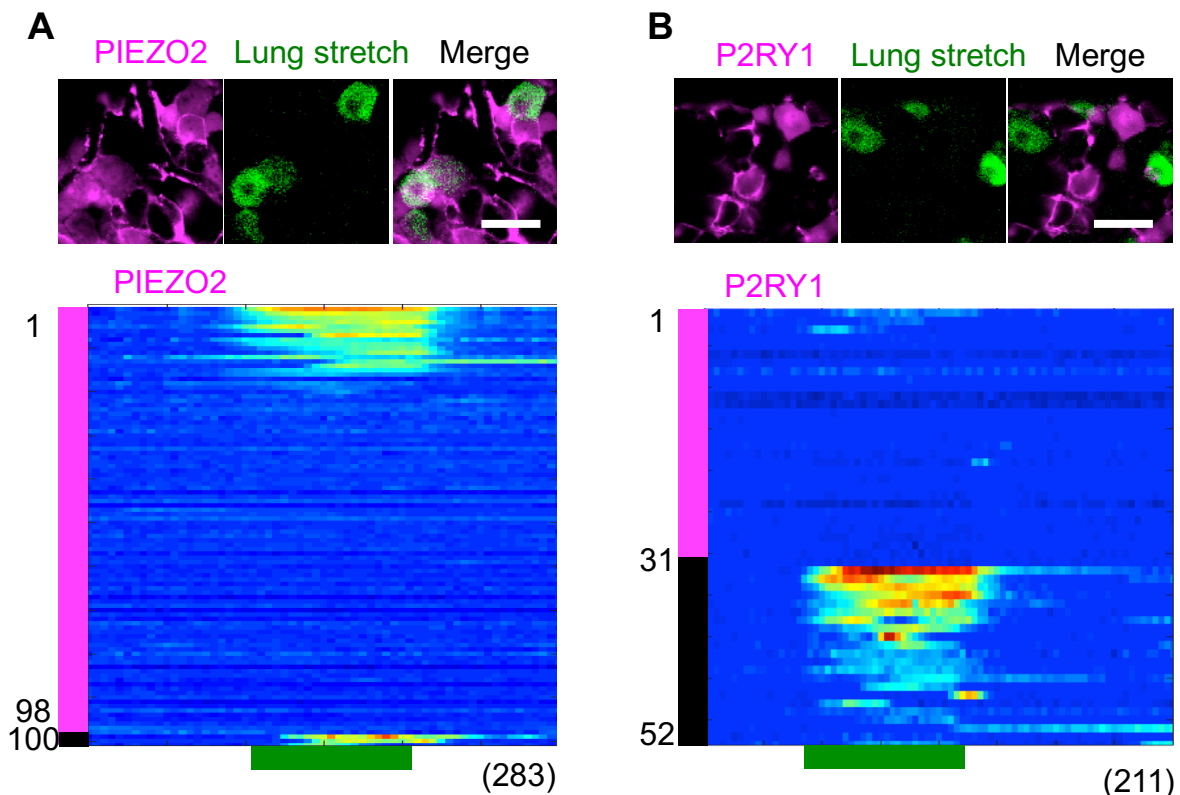


Figure 3. PIEZO2 neurons, but not P2RY1 neurons contain lung mechanoreceptors. (A) Representative images and time-resolved responses of 100 sensory neurons, ($\Delta F/F$, color scale) in response to lung stretch (green bar, 15 seconds). Nearly all lung-stretch responsive neurons are contained with the PIEZO2 neuron population. (B) Representative images and time-resolved responses of 52 sensory neurons, ($\Delta F/F$, color scale) in response to lung stretch (green bar, 15 seconds). None of the lung-stretch responsive neurons are contained with the P2RY1 neuron population. Scale bars, 50 μm .

In contrast, in P2RY1 experiments, twenty-three neurons were identified as responsive to lung stretch (11%), a proportion of the total ganglion somewhat higher than prior estimates of the size of the lung stretch population. Of these 23 lung stretch responsive neurons, 2 were positive for tdTomato (8.6%), though the response amplitudes of these two neurons were markedly reduced compared to tdTomato negative responsive neurons. From these data, we conclude that the P2RY1 neuron population largely does not include lung-stretch sensitive cells (Figure 3B).

In PIEZO2 experiments, thirty-one neurons were identified as responsive to stomach stretch, a proportion of the ganglion (13.1%) consistent with prior estimates of the size of the stomach-stretch responsive population. Of these 31 stomach stretch responsive neurons, using standard cut-offs to define responders versus non-responders, 18 (52.9%) were positive for tdTomato (Figure 4A). An independent-samples t-test was conducted to compare the mean response amplitude, expressed as percent change from baseline, during stomach stretch in tdTomato positive versus tdTomato negative stomach-stretch responsive neurons. There was a significant difference in the response amplitudes for tdTomato positive ($M = 66$, $SEM = 16$) and tdTomato negative ($M = 11$, $SEM = 5$) neurons; $t(29) = 2.83$, $p = 0.008$. Therefore, though by standard definitions for responsive versus non-responsive neurons, only half of stomach-stretch responsive cells are tdTomato positive, the tdTomato positive neurons were much more strongly responsive than the tdTomato negative neurons. Conversely, 18 of 84 (21%) tdTomato positive neurons were stomach stretch responsive. From these data we conclude that most strongly responsive stomach stretch sensitive neurons have expressed Piezo2, and that stomach-stretch responsive neurons account for another one-fifth of neurons that have expressed Piezo2.

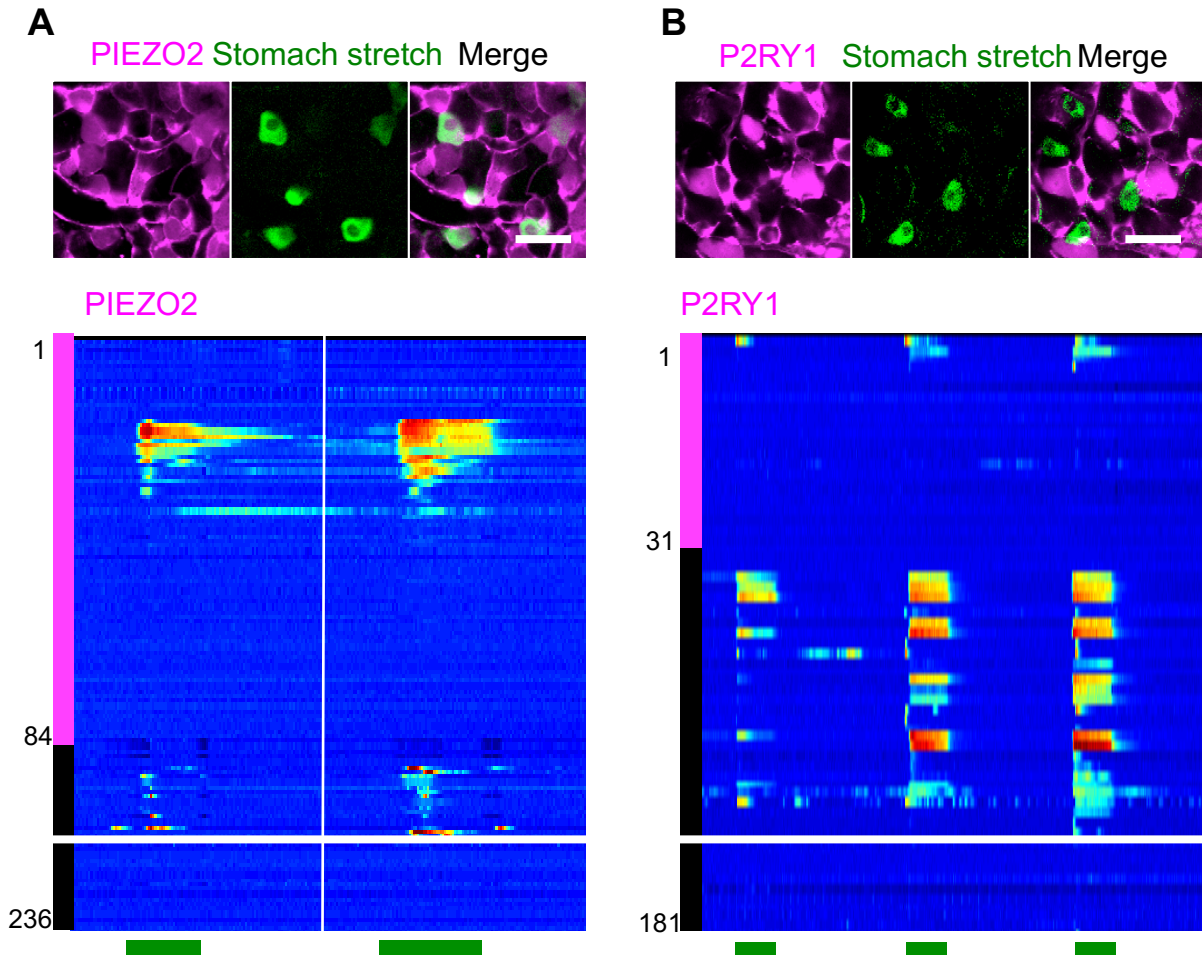


Figure 4. PIEZO2 neurons, but not P2RY1 neurons contain stomach mechanoreceptors. (A) Representative images and time-resolved responses of 236 sensory neurons, ($\Delta F/F$, color scale) in response to stomach stretch. Nearly all lung-stretch responsive neurons are contained with the PIEZO2 neuron population. (B) Representative images and time-resolved responses of 181 sensory neurons, ($\Delta F/F$, color scale) in response to stomach stretch. None of the stomach-stretch responsive neurons are contained with the P2RY1 neuron population. All scale bars, 50 μm . Green bars under the raster plots indicate time of application of stretch stimuli (Piezo2 20 and 30 seconds, P2ry1 30 seconds).

Finally, though one of the stomach stretch preparations failed in P2RY1 experiments, data was analyzed from two of the three animals tested, yielding a total of 181 electrically responsive neurons. Of these 181 neurons, 32 (17.7%) were responsive to stomach stretch, a proportion similar to prior estimates of the size of the stomach stretch sensitive population. Of the 32 stomach stretch responsive neurons, 4 (13%) were positive for tdTomato (Figure 4B). From these data we conclude that the majority of stomach stretch sensitive neurons have never expressed P2ry1.

Conclusions

Neurons that have expressed Piezo2 at some point in their lifetime encompass stomach and lung mechano-sensitive populations. In contrast, neurons that have expressed P2ry1 in their lifetime are not responsive to stomach or lung mechanical stimuli. These findings have two key implications.

First, these data support the hypothesis that Piezo2 could be the molecular mechanosensor. As a corollary, such a conclusion would also suggest that the neurons themselves could be the primary mechanosensor because they are marked by expression of a known molecular mechanosensor. Further experiments are required, however, to demonstrate the relevance of the Piezo2 molecule itself. While some data already support the role of Piezo2 in lung mechanosensation, nothing is known about Piezo2 in gastric mechanosensation.

Second, these data support the conclusion the Piezo2-positive, P2ry1-negative neurons contain the relevant lung-stretch responsive population. This observation is important for two reasons. First, it is a clear demonstration that P2RY1 neurons are not responsible for the Hering Breuer reflex, begging the question what A-fibers that selectively innervate neuroepithelial bodies and who can induce complete mouse apnea are doing. P2ry1 is a unique molecular handle on an unanticipated vagal neuron subset. Second, because lung-stretch responsive neurons only cover a subset of PIEZO2 neurons, additional genetic markers are required to more precisely define the lung stretch subset. P2ry1 can therefore serve in future experiments, such as in analysis of single-cell data, to restrict investigation into Piezo2-positive, P2ry1-negative neuron types. Such experiments might reveal critical markers or manipulable features of lung-stretch sensitive neuron subsets to be exploited in the future.

Experiment 2: In vivo imaging of neurons that express Piezo2 in the adult

Introduction

Neurons that have expressed Piezo2 at some point in their development contain nearly all the lung and stomach stretch responders. However, a critical shortcoming of lineage-tracing experiments is that they do not distinguish between historic, developmental expression and active functional expression in the adult. If Piezo2 were the mechanosensor itself, one would also additionally predict that mechanosensitive neurons express Piezo2 not only at some time during development, but also that they express Piezo2 in adulthood. To test this hypothesis requires an experimental paradigm in which neurons that express Piezo2 in adulthood are selectively labeled, and in which their response properties can be recorded to stretch stimuli.

Methods

We generated the double knock-in mouse line Piezo2-ires-Cre; Rosa26-GCaMP3, and used adeno-associated viruses to deliver flex-tdTomato vectors to all nodose sensory neurons. This resulted in expression of tdTomato only in neurons expressing Piezo2-Cre at the time of injection in adulthood. Response properties of labeled neurons could then be recorded using in vivo calcium imaging as in prior experiments.

Given concerns about the impact of viral injections on neuron health and responsiveness, the same experiments were performed using Glp1r-ires-Cre; Rosa26-GCaMP3 animals as potential positive controls. GLP1R neurons had previously been shown to include the stomach-stretch responsive neuron population³³.

Adeno-associated virus injections were performed as described previously^{33,77}. Briefly, mice are anesthetized, the left nodose ganglion surgically exposed, and AAV mixed with Fast Green dye is injected into the body of the ganglion. Injections are considered grossly successful when the ganglion body fills with blue dye. The incision in the neck is

closed and the animals allowed to recover. Imaging experiments were performed 6-7 days following injections in hopes of preserving neuron viability while achieving reasonable amounts of infection and construct expression.

Results

In Piezo2 animals, 631 electrically responsive neurons were analyzed (n = 7 animals). Of these 631 neurons, 45 were tdTomato positive, suggesting a combined infection and expression efficiency of 7.1%. When the same analysis was performed based only upon morphological identification of cell bodies rather than on responsiveness to electrical stimulation, 811 neurons were identified of which 72 were tdTomato positive (8.8% efficiency). The similarity of tdTomato expression frequency in all neurons versus all electrically responsive neurons suggests that tdTomato expression was not impairing gross neuron responsiveness.

In Glp1r animals, 441 electrically responsive neurons were analyzed (n = 4 animals). Of these 441 neurons, 40 were tdTomato positive, suggesting a combined infection and expression efficiency of 9.0%. This efficiency is concordant with the observation that in situ hybridization for *Piezo2* and *Glp1r* in adult mouse nodose ganglia results in labeling neuronal subsets of similar size.

We first examined the degree of overlap between tdTomato-expressing neurons and stomach stretch responsiveness. In Glp1r experiments, 71 neurons in total responded to stomach stretch. Of the 40 tdTomato-positive neurons in Glp1r animals, 18 (45%) were responsive to stomach stretch (Figure 5A). A Chi-squared test for independence showed that there was a significant relationship between tdTomato expression and stretch responsiveness, $\chi^2(2, N = 441) = 27.203, p < 0.01$ (Figure 5B). This result is in accord with the earlier observation that GLP1R neurons contain nearly all the stomach stretch responsive neurons, and that adult labeling of GLP1R neurons labels nearly all IGLE-type endings in the stomach³³. These results serve as an important proof of concept and positive control.

In Piezo2 animal experiments, 54 of the 631 neurons analyzed were responsive to stomach stretch (8.6%). Of these stomach stretch responders, 5 (9.2%) were tdTomato

positive (Figure 5A). These data suggest two observations. First, a subset of adult Piezo2-expressing neurons can respond to stomach stretch. However, we would further predict that if Piezo2 is the relevant stomach mechanosensor, there should be greater-than-chance co-occurrence of tdTomato expression and stomach stretch responsiveness. We performed a Chi-squared analysis, and found that there was no relationship between stomach stretch and adult Piezo2 expression, $X^2(2, N = 631) = 0.40, p = 0.53$ (Figure 5B). These data do not support the hypothesis that Piezo2 is the relevant adult gastrointestinal mechanosensor.

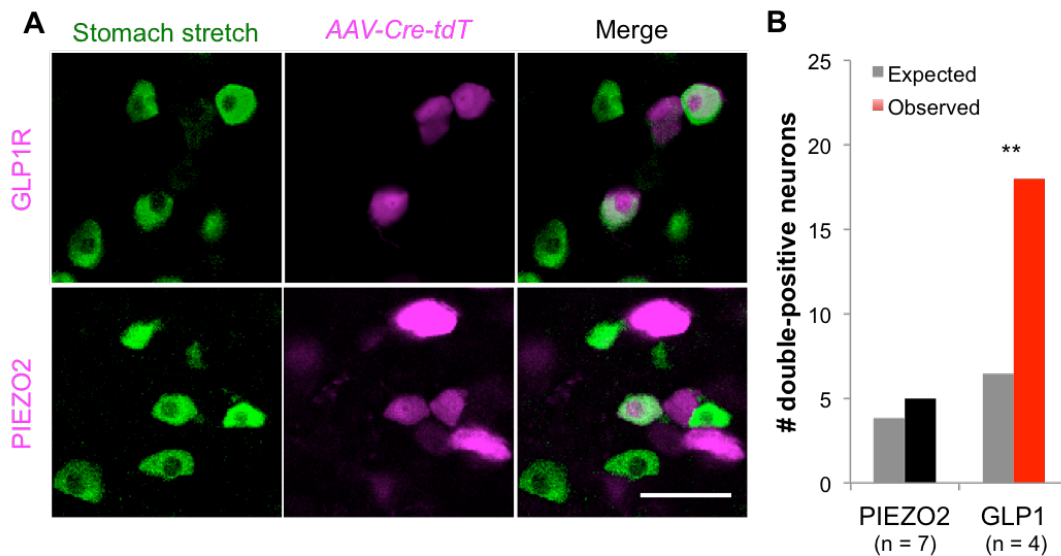


Figure 5. Expression of *Piezo2* in adulthood does not preferentially label stomach stretch sensitive neurons. (A) Representative images of neuron responses to stomach stretch (green) in *Glp1r-iresCre AAV-lox-tdTomato* and *Piezo2-iresCre AAV-lox-tdTomato* neurons (pink). Scale bar, 50 μm . (B) Plot of the observed number of tdTomato and stomach stretch double-positive neurons (PIEZO2, black; GLP1R, red) versus the expected number of neurons calculated based on infection and response rates (gray). ** $p < 0.01$ for X^2 test for independence.

We next examined the degree of overlap between tdTomato-expressing neurons and lung stretch responsiveness. Only two *Glp1r* animals had lung-stretch stimuli administered, resulting in analysis of 169 electrically responsive neurons. Seventeen neurons were responsive to lung stretch (10%), a response rate similar to prior experimental paradigms. None of these responsive neurons were tdTomato positive, consistent with prior work showing no overlap between GLP1R neuron subsets labeled with genetic lineage-tracing methods, and lung-stretch responsive subsets.

In *Piezo2* experiments, of the 631 electrically responsive neurons, 29 were responsive to lung stretch (4.6%), similar to previously reported rates of lung-stretch

responsiveness. Of these 29 lung stretch responsive neurons, 3 (10.3%) were tdTomato positive. A Chi-squared analysis showed there was no relationship between lung stretch responsiveness and tdTomato expression, $\chi^2 (2, N = 631) = 0.47, p = 0.49$. This result is surprising in light of the findings that knockout of Piezo2 impacts the Hering-Breuer reflex and whole-nerve recordings of the vagus in response to lung stretch.

Conclusions

The relationship between Glp1r-driven AAV-tdTomato expression and stomach stretch responsiveness confirms that stomach-stretch responsive neurons express Glp1r in adulthood. More importantly, this observation suggests that viral infection and in vivo imaging can be compatible techniques in this paradigm. However, the finding that there was no relationship between adult Piezo2-driven tdTomato expression and stomach stretch responsiveness casts doubt on the hypothesis that Piezo2 is the relevant molecular mechanosensor in stomach stretch. Rather, this result might suggest that Piezo2 plays an important developmental role in the formation of IGLs, but that its expression is not preserved into adulthood in this neuron population.

However, the observation that adult Piezo2-driven tdTomato expression and lung stretch responsiveness are not related is surprising. Knockout of Piezo2 from birth in the neuron subset imaged in these experiments abolishes whole-nerve responses to lung stretch. It is possible that an insufficient number of neurons was queried in this paradigm to reveal a relationship; lung-stretch responsive cells are much more rare than stomach-stretch responders. Despite multiple imaging preparations, this result depends heavily on data from less than 30 neurons. Furthermore, the robustness of neuron populations to viral infection may differ depending on neuron type, making this experiment suitable to examine stomach-stretch, but not lung-stretch sensitive subsets.

Alternatively, if lung-stretch responsive neurons truly do not express Piezo2 in adulthood, it would suggest that Piezo2 in the neurons themselves is not critical for lung mechanosensation. Perhaps the expression of Piezo2 in non-neuronal elements, such as its expression in the nodose satellite cells or in target organs, is sufficient to confer mechanosensitivity. Drivers used to knock out Piezo2 in prior experiments are not fully

nodose-neuron specific. Similarly, an additional alternative explanation is that Piezo2 plays an important developmental role in lung stretch sensitive afferents and/or their surrounding structures such that its loss would confer mechano-insensitivity without Piezo2 being the actual mechanoreceptor.

Experiment 3: Detection of stretch stimuli in Piezo2 knock-out ganglia

Introduction

The hypothesis that Piezo2 acts as the mechanosensor in vagal sensory afferents furthermore suggests two additional predictions. First, loss of expression of Piezo2 should result in the loss of mechanically evoked responses. Second, if the neurons are the direct mechanosensors, the selective loss of Piezo2 in the neurons themselves but not in other tissues should be sufficient to abolish responses. To test these predictions requires an experimental paradigm in which Piezo2 expression is disrupted selectively in the nodose ganglion neurons, and in which response properties can still be recorded.

Methods

Using a series of mouse crosses, we generated Piezo2^{fl/fl}-GCaMP3*, Piezo2^{fl/wt}-GCaMP3*, and Piezo2^{wt/wt}-GCaMP3* animals. An adeno-associated virus containing a CAG-Cre-mCherry construct was purchased from SignaGen laboratories (*AAV1-CAG-Cre-mCherry*, SL101117). Infection with this vector is intended to induce the expression of a Cre recombinase and mCherry fusion allele to generate red nuclear fluorescence in every neuron also expressing Cre. Expression of Cre recombinase in cells containing a floxed Piezo2 allele would result in genetic knockout of Piezo2. Imaging experiments were

performed 14-21 days after AAV injections in hopes of providing sufficient time for knockdown of Piezo2 expression. Successful expression of Cre, and excision of the Piezo2 allele were confirmed using PCR of ganglia collected after completion of imaging experiments.

Results

Two to three weeks following injection of AAV1-CAG-Cre-mCherry, nodose ganglia demonstrated widespread and robust expression of tdTomato in the infected ganglion, but not in the uninfected contralateral ganglion. The red fluorescence was localized to the cell nucleus, concordant with the fluorescent protein being tagged to nucleus-localized Cre recombinase. In the five injected animals, 278 electrically responsive neurons were analyzed, of which 186 (67%) contained a mCherry-positive nucleus, suggesting high infection efficiency in these experiments (Figure 6A). PCR of ganglion DNA extracted after imaging experiments showed positive reactions for Cre recombinase from infected, but not from uninfected ganglia. Furthermore, PCR reactions specific for the sequence of the knockout Piezo2 allele were positive only in infected ganglia from mice carrying at least one floxed Piezo2 allele (Figure 6B). These results suggest not only that Cre was successfully expressed, but also that it was functional and excised the floxed region of Piezo2.

Of five animals successfully tested, two were Piezo2^{fl/wt}, meaning that Piezo2 expression from one allele should always be preserved despite expression of Cre. In these animals, 107 electrically responsive neurons were analyzed. Of these 107 neurons, 7 (6.5%) were responsive to lung stretch, 5 of which were mCherry positive and 2 of which were mCherry negative. Furthermore, 19 (17.8%) were stomach stretch responsive, of which 14 were mCherry positive and 5 were mCherry negative. Therefore, Cre expression did not abolish mechanosensitive responses in nodose sensory neurons (Figure 7A). Chi-squared analysis showed there was no relationship between lung stretch responsiveness and tdTomato expression, $X^2(2, N = 107) = 0.90, p = 0.34$, nor between stomach stretch responsiveness and mCherry expression in animals, $X^2(2, N = 107) = 1.88, p = 0.17$. These data suggest that injection and construct expression itself does not impact mechanical sensitivity of vagal sensory neurons.

The remaining three animals tested were Piezo2^{fl/fl} animals, meaning that neurons expressing mCherry in these animals also have excision of both copies of the floxed Piezo2 genetic sequence. In these animals, 171 electrically responsive neurons were analyzed. Of these 171 neurons, 25 (14%) were stomach-stretch responsive, of which 14 were mCherry positive and 11 were mCherry negative. Furthermore, 4 (2.3%) were lung stretch responsive, of which 2 were mCherry positive and 2 were mCherry negative. Therefore, even when both Piezo2 alleles were floxed, neurons expressing Cre recombinase maintained their ability to respond to mechanical stimuli (Figure 7A). A Chi-squared analysis showed there was no relationship between stomach stretch responsiveness and mCherry expression in Piezo2-floxed animals, $X^2(2, N = 171) = 0.0002, p = 0.98$, nor between lung stretch responsiveness and mCherry expression, $X^2(2, N = 171) = 0.07, p = 0.80$. Similarly, there was no attenuation in stomach stretch response amplitude in mCherry-positive neurons in Piezo2^{fl/fl} animals (Figure 7B). Rather, mCherry-positive neurons had a slightly greater response amplitude ($M = 2.1, SD = 1.3$) than mCherry-negative neurons ($M = 1.0, SD = 1.02$), $t(22) = 0.481, p = 0.03$. Too few lung stretch responsive neurons were present in these preparations for rigorous statistical analysis of response amplitudes, particularly given the small number of animals tested.

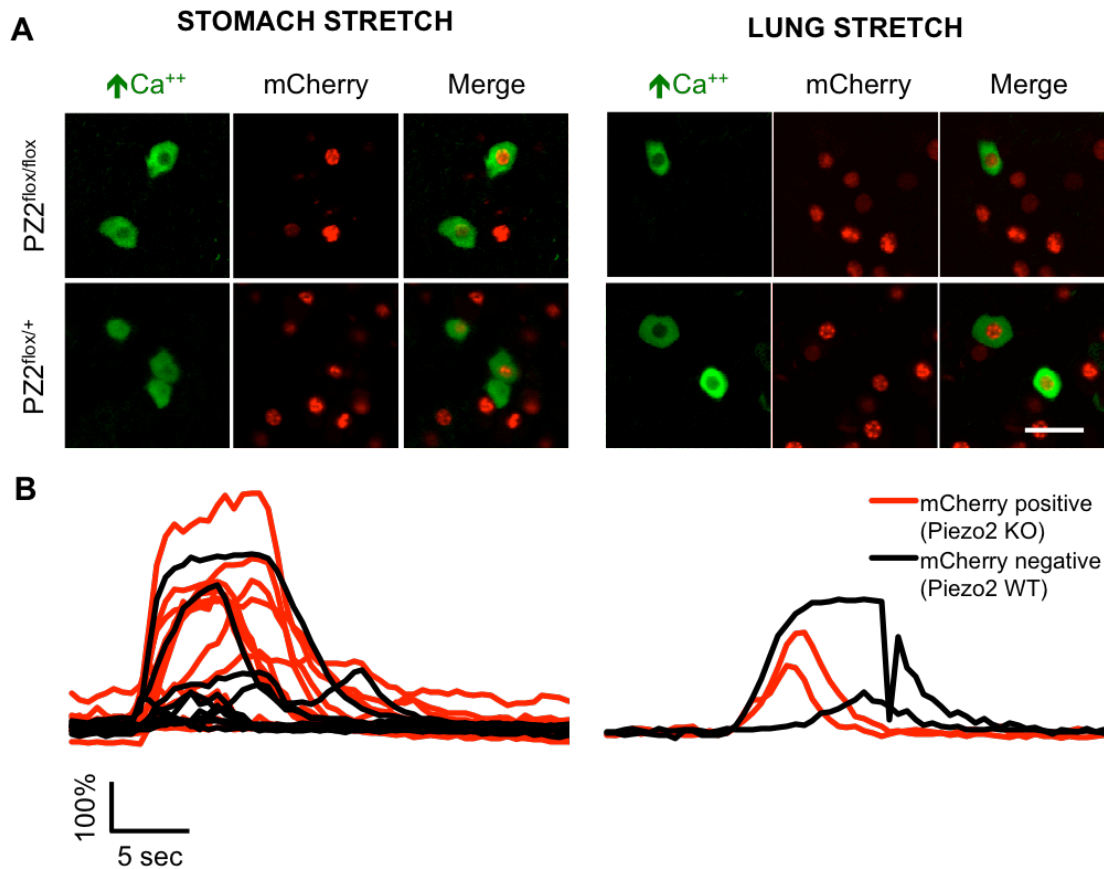


Figure 7. Neuron-specific, adult deletion of *Piezo2* does not abolish mechanical responses. (A) Representative images of preserved stomach and lung stretch responses in mCherry-positive and negative neurons in *Piezo2*^{fl/fl} and *Piezo2*^{fl/wt} animals. Scale bar, 50 μ m. (B) Response amplitudes for all stomach stretch (left) and lung stretch (right) responsive neurons in *Piezo2*^{fl/fl} animals. Traces from neurons that express mCherry are in red, while traces from neurons that do not express mCherry are in black.

Conclusions

The lack of relationship between *Piezo2* excision and either stomach or lung stretch casts further doubt on the role of *Piezo2* on lung and stomach mechanosensation in vagal sensory afferents. However, one technical point limits enthusiasm for the strength of conclusions to be drawn in this experiment. While genomic excision of the *Piezo2* exons could be confirmed grossly by whole-ganglion PCR, this validation provides only a proxy indication that protein levels of *Piezo2* are altered using this experimental manipulation. For example, the *Piezo2* knockout-specific PCR reaction could be positive in cases of excision of the floxed *Piezo2* region in only an incomplete subset of neurons. Alternatively,

even if knockout were complete at the genomic level, the durability of expressed Piezo2 protein is unknown, and may extend beyond the 2-3 weeks between infection and imaging utilized in this experimental paradigm. However, intriguingly, the only other experiment to knock down Piezo2 in adult animals generated reductions in skin sensitivity within one week of induction of genomic excision of the floxed region of Piezo2⁶⁹, suggesting the 2-3 week window used in these experiments should be sufficient. Unfortunately, tools to evaluate protein expression, and specifically protein expression at distal sensory terminals within target organs, are lacking. Interpretation of results must therefore necessarily be constrained with this shortcoming in mind. The absence of a relationship is a negative result that could reflect true biology, or a technical hurdle.

With incomplete validation of Piezo2 protein expression knockdown in mind as a prominent technical short-coming for data interpretation, these data are not concordant with the hypothesis that vagal sensory neuron Piezo2 is the sole and necessary mechanosensor in either stomach or lung stretch. This conclusion agrees with the lack of relationship between the adult expression of Piezo2 and stomach stretch in prior experiments, supporting the notion that Piezo2 does not play a role in the adult gastric mechanosensitive neuron population.

The lack of relationship between neuronal Piezo2 knockout and lung stretch responsiveness, however, is surprising. The single prior experiment to suggest Piezo2 knockout in adults alters respiratory dynamics and attenuates the Hering Breuer reflex used a tamoxifen-dependent Advillin-Cre driver to delete Piezo2 from vagal and dorsal root ganglion neurons⁶⁹. The knockout mice had 30% larger tidal volumes, and reached peak expiratory flow faster than wild-type controls. These animals also had lower whole vagal nerve activity during lung inflation. One difference between this experiment and virally mediated knockdown is that Advillin-Cre also drives Piezo2 knockout outside the vagus (e.g. in the dorsal root ganglia), which could impact respiratory dynamics. However, this would not directly explain lower vagal whole-nerve recording lung stretch response amplitudes. In addition to tamoxifen-induced Advillin-Cre-driven Piezo2 knockout, the driver Phox2b was used to delete Piezo2 from birth in nodose neurons and glia. Knockout from birth resulted in abolition of the Hering Breuer reflex and vagus nerve responses to lung inflation. However, experiments that knock out a gene from birth cannot distinguish

between developmental and adult impact of gene loss. Therefore, the possibility remains that, as in Merkel cells in the skin, non-vagal Piezo2 expression plays an important role in Piezo mechanotransduction, and that knockout specifically in adult vagal sensory neurons is insufficient to abolish lung stretch mechanosensitivity.

Summary

Detection of mechanical forces within the body plays a critical role in regulation of organism physiology. We investigated whether Piezo2, a recently identified mammalian mechanosensor, could play a role in detection of internal mechanosensory cues. We found that lineage tracing of neurons that have expressed Piezo2 labeled the large majority of lung and stomach mechanosensitive neuron populations in the nodose ganglion of the vagus nerve. However, neurons that expressed Piezo2 in adulthood did not preferentially label mechanosensitive populations. In addition, adult and nodose neuron specific Piezo2 knockout failed to abolish mechanosensitive responses in nodose sensory neurons, though conclusions from this experiment are limited by technical concerns. These data in aggregate suggest Piezo2 may not be the sole mechanosensor within internal sensory systems, and furthermore raise the possibility that extra-neural Piezo2 could play an important role in these systems as it does in the skin, or that Piezo2 plays an important developmental role. Further experimentation such as 1) using alternative methods to knock out Piezo2 from vagal sensory neurons and associated tissues, 2) evaluation of adult PIEZO2 neuron anatomy in the periphery, and 3) investigation into the role of Piezo2 in the cardiovascular system, would shed intriguing light onto the role of PIEZO2 neurons, and the role of Piezo2 expression in internal mechanosensation.

Bibliography

1. Foley, J. O. & DuBois, F. S. Quantitative studies of the vagus nerve in the cat. I. The ratio of sensory to motor fibers. *Journal of Comparative Neurology* **67**, 49–67 (1937).

2. Sawchenko, P. E. Central connections of the sensory and motor nuclei of the vagus nerve. *J. Auton. Nerv. Syst.* **9**, 13–26 (1983).
3. Saper, C. B. The central autonomic nervous system: conscious visceral perception and autonomic pattern generation. *Annu. Rev. Neurosci.* **25**, 433–469 (2002).
4. Rinaman, L., Card, J. P., Schwaber, J. S. & Miselis, R. R. Ultrastructural demonstration of a gastric monosynaptic vagal circuit in the nucleus of the solitary tract in rat. *Journal of Neuroscience* **9**, 1985–1996 (1989).
5. Janowitz, H. & Grossman, M. I. Some factors affecting the food intake of normal dogs and dogs with esophagostomy and gastric fistula. *Am. J. Physiol. Regul. Integr. Comp. Physiol.* **159**, 143–148 (1949).
6. Share, I., Martyniuk, E. & Grossman, M. I. Effect of prolonged intragastric feeding on oral food intake in dogs. *Journal of Physiology* **169**, 229–235 (1952).
7. Phillips, R. J. & Powley, T. L. Gastric volume rather than nutrient content inhibits food intake. *Am. J. Physiol.* **271**, R766–9 (1996).
8. Powley, T. L. & Phillips, R. J. Gastric satiation is volumetric, intestinal satiation is nutritive. *Physiology & Behavior* **82**, 69–74 (2004).
9. Phillips, R. J. & Powley, T. L. Gastric volume detection after selective vagotomies in rats. *Am. J. Physiol.* **274**, R1626–38 (1998).
10. Gonzalez, M. F. & Deutsch, J. A. Vagotomy abolishes cues of satiety produced by gastric distension. *Science* **212**, 1283–1284 (1981).
11. Walls, E. K., Phillips, R. J., Wang, F. B., Holst, M. C. & Powley, T. L. Suppression of meal size by intestinal nutrients is eliminated by celiac vagal deafferentation. *Am. J. Physiol.* **269**, R1410–9 (1995).
12. Yox, D. P., Stokesberry, H. & Ritter, R. C. Vagotomy attenuates suppression of sham feeding induced by intestinal nutrients. *Am. J. Physiol.* **260**, R503–8 (1991).
13. Ogawa, N. *et al.* The vagal afferent pathway does not play a major role in the induction of satiety by intestinal fatty acid in rats. *Neuroscience Letters* **433**, 38–42 (2008).
14. Sclafani, A. & Lucas, F. Abdominal vagotomy does not block carbohydrate-conditioned flavor preferences in rats. *Physiology & Behavior* **60**, 447–453 (1996).
15. Colquitt JL, P. K. L. E. F. G. Surgery for weight loss in adults (Review). 1–243 (2013).
16. Ponce, J. *et al.* The REDUCE pivotal trial_ a prospective, randomized controlled pivotal trial of a dual intragastric balloon for the treatment of obesity. 1–8 (2015). doi:10.1016/j.soard.2014.12.006
17. Moura, D. *et al.* Effectiveness of intragastric balloon for obesity_ A systematic review and meta-analysis based on randomized control trials. *Surgery for Obesity and Related Diseases* **12**, 420–429 (2016).
18. Dixon, J. B. *et al.* Adjustable gastric banding and conventional therapy for type 2 diabetes: a randomized controlled trial. *JAMA* **299**, 316–323 (2008).
19. Favretti, F. *et al.* Laparoscopic adjustable gastric banding in 1,791 consecutive obese patients: 12-year results. *Obes Surg* **17**, 168–175 (2007).
20. Sjöström, L. *et al.* Effects of bariatric surgery on mortality in Swedish obese subjects. *N. Engl. J. Med.* **357**, 741–752 (2007).
21. Paintal, A. S. A study of gastric stretch receptors; their role in the peripheral mechanism of satiation of hunger and thirst. *Journal of Physiology* **126**, 255–270 (1954).

22. Iggo, A. Tension receptors in the stomach and the urinary bladder. *J. Physiol. (Lond.)* **128**, 593–607 (1955).
23. Iggo, A. GASTROINTESTINAL TENSION RECEPTORS WITH UNMYELINATED AFFERENT FIBRES IN THE VAGUS OF THE CAT. *Quarterly Journal of Experimental Physiology and Cognate Medical Sciences* **42**, 130–143 (1957).
24. Slattery, J. A., Page, A. J., Dorian, C. L., Brierley, S. M. & Blackshaw, L. A. Potentiation of mouse vagal afferent mechanosensitivity by ionotropic and metabotropic glutamate receptors. *J. Physiol. (Lond.)* **577**, 295–306 (2006).
25. Ashley Blackshaw, L., Grundy, D. & Scratcherd, T. Involvement of gastrointestinal mechano- and intestinal chemoreceptors in vagal reflexes" an electrophysiological study. *J. Auton. Nerv. Syst.* **18**, 1–10 (2002).
26. Blackshaw, L. A., Page, A. J. & Partosoedarso, E. R. Acute effects of capsaicin on gastrointestinal vagal afferents. *Neuroscience* **96**, 407–416 (2000).
27. Jin, Y.-H., Takemura, M., Furuyama, A. & Yonehar, N. Receptors Inhibit Mechanosensitivity of Primary Afferent Endings. *Pharmacology* 1–6 (1999). doi:10.5772/34100
28. Zagorodnyuk, V. P., Chen, B. N., Costa, M. & Brookes, S. J. H. Mechanotransduction by intraganglionic laminar endings of vagal tension receptors in the guinea-pig oesophagus. *J. Physiol. (Lond.)* **553**, 575–587 (2004).
29. Regehr, B. L. S. A. W. G. TIMING OF SYNAPTIC TRANSMISSION. *Annu. Rev. Physiol.* **61**, 521–542 (1999).
30. Bennett, M. & Zukin, S. Electrical Coupling and Neuronal Synchronization in the Mammalian Brain. *Neuron* **41**, 495–511 (2004).
31. Zagorodnyuk, V. P. & Brookes, S. J. Transduction sites of vagal mechanoreceptors in the guinea pig esophagus. *Journal of Neuroscience* **20**, 6249–6255 (2000).
32. Zagorodnyuk, V. P., Chen, B. N. & Brookes, S. J. Intraganglionic laminar endings are mechano-transduction sites of vagal tension receptors in the guinea-pig stomach. *J. Physiol. (Lond.)* **534**, 255–268 (2001).
33. Williams, E. K. *et al.* Sensory Neurons that Detect Stretch and Nutrients in the Digestive System. *Cell* **166**, 209–221 (2016).
34. NONIDEZ, J. F. Afferent nerve endings in the ganglia of the intermuscular plexus of the dog's oesophagus. *J. Comp. Neurol.* **85**, 177–189 (1946).
35. Neuhuber, W. L. Sensory vagal innervation of the rat esophagus and cardia: a light and electron microscopic anterograde tracing study. *J. Auton. Nerv. Syst.* **20**, 243–255 (1987).
36. Wang, F. B. & Powley, T. L. Topographic inventories of vagal afferents in gastrointestinal muscle. *J. Comp. Neurol.* **421**, 302–324 (2000).
37. Berthoud, H. R. & Powley, T. L. Vagal afferent innervation of the rat fundic stomach: morphological characterization of the gastric tension receptor. *J. Comp. Neurol.* **319**, 261–276 (1992).
38. Berthoud, H. R., Patterson, L. M., Neumann, F. & Neuhuber, W. L. Distribution and structure of vagal afferent intraganglionic laminar endings (IGLEs) in the rat gastrointestinal tract. *Anatomy and Embryology* **195**, 183–191 (1997).
39. fox, E. A., Phillips, R. J., Martinson, F. A., Baronowsky, E. A. & Powley, T. L. Vagal afferent innervation of smooth muscle in the stomach and duodenum of the mouse: morphology and topography. *J. Comp. Neurol.* **428**, 558–576 (2000).

40. Powley, T. L. *et al.* Ultrastructural evidence for communication between intramuscular vagal mechanoreceptors and interstitial cells of Cajal in the rat fundus. *Neurogastroenterology & Motility* **20**, 69–79 (2008).
41. Widdicombe, J. Reflexes from the lungs and airways: historical perspective. *J. Appl. Physiol.* **101**, 628–634 (2006).
42. Breuer, J. The self-steering of respiration through the Nervus Vagus, translated by E. Ullman. *Breathing Hering-Breuer Centenary Symposium Ciba Foundation Symposium*, 357–394 (1970).
43. Head, H. On the Regulation of Respiration: PART I. Experimental. *J. Physiol. (Lond.)* **10**, 1–152.53 (1889).
44. Head, H. On the Regulation of Respiration: Part II. Theoretical. *J. Physiol. (Lond.)* **10**, 279–290 (1889).
45. Cross, K. W., KLAUS, M., TOOLEY, W. H. & WEISSER, K. The response of the new-born baby to inflation of the lungs. *J. Physiol. (Lond.)* **151**, 551–565 (1960).
46. Guz, A., Noble, M. I. M., Trenchard, D., Cochrane, H. L. & Makey, A. R. Studies on the vagus nerve in man: their role in respiratory and circulatory control. *Clinical Science* 293–304 (1964).
47. Dejours, P., RAYNAUD, J., MONZEIN, P. & BECHTEL, Y. [Study of the Hering-Breuer inspiration inhibitor reflex in man during natural sleep]. *J. Physiol. (Paris)* **54**, 320–321 (1962).
48. Guz, A., Noble, M. I. M., Widdicombe, J. G., Trenchard, D. & Mushin, W. W. The effect of bilateral block of vagus and glossopharyngeal nerves on the ventilatory response to CO₂ of conscious man. *Respiration Physiology* **1**, 206–210 (1966).
49. Guz, A. *et al.* The role of vagal and glossopharyngeal afferent nerves in respiratory sensation, control of breathing and arterial pressure regulation in conscious man. *Clinical Science* **30**, 161–170 (1966).
50. Anrep, G. V., Pascual, W. & Rossler, R. Respiratory variations of the heart rate - I—The reflex mechanism of the respiratory arrhythmia. *Proceedings of the Royal Society B* **119**, 191–213 (1936).
51. Bainbridge, F. A. The relation between respiration and the pulse-rate. *J. Physiol. (Lond.)* **54**, 192–202 (1920).
52. De Burgh Daly, M., Hazzledine, J. L. & Ungar, A. The reflex effects of alterations in lung volume on systemic vascular resistance in the dog. *J. Physiol. (Lond.)* **188**, 331–351 (1967).
53. Looga, R. Reflex cardiovascular responses to lung inflation: a review. *Respiration Physiology* **109**, 95–106 (1997).
54. Adrian, E. D. Afferent impulses in the vagus and their effect on respiration. *J. Physiol. (Lond.)* **79**, 332–358 (1933).
55. KNOWLTON, G. C. & LARRABEE, M. G. A unitary analysis of pulmonary volume receptors. *Am. J. Physiol.* **147**, 100–114 (1946).
56. Bartlett, D., Jeffery, P., Sant'Ambrogio, G. & Wise, J. C. Location of stretch receptors in the trachea and bronchi of the dog. *J. Physiol. (Lond.)* **258**, 409–420 (1976).
57. Widdicombe, J. G. Receptors in the trachea and bronchi of the cat. *J. Physiol. (Lond.)* **123**, 71–104 (1954).
58. Bartlett, D. & Sant'Ambrogio, G. Effects of local and systemic hypercapnia on the discharge of stretch receptors in the airways of the dog. *Respiration Physiology* **26**,

- 91–99 (1976).
59. Sheldon, M. I. & Green, J. F. Evidence for pulmonary CO₂ chemosensitivity: effects on ventilation. *J Appl Physiol Respir Environ Exerc Physiol* **52**, 1192–1197 (1982).
 60. Matsumoto, S., Takahashi, T., Tanimoto, T., Saiki, C. & Takeda, M. Effects of potassium channel blockers on CO₂-induced slowly adapting pulmonary stretch receptor inhibition. *The Journal of Pharmacology and Experimental Therapeutics* **290**, 974–979 (1999).
 61. Ho, C. Y., Gu, Q., Lin, Y. S. & Lee, L. Y. Sensitivity of vagal afferent endings to chemical irritants in the rat lung. *Respiration Physiology* **127**, 113–124 (2001).
 62. Karlsson, J. A., Sant'Ambrogio, G. & Widdicombe, J. Afferent neural pathways in cough and reflex bronchoconstriction. *J. Appl. Physiol.* **65**, 1007–1023 (1988).
 63. Widdicombe, J. Airway receptors. *Respiration Physiology* **125**, 3–15 (2001).
 64. Pisarri, T. E., Jonzon, A., COLERIDGE, H. M. & COLERIDGE, J. C. Vagal afferent and reflex responses to changes in surface osmolarity in lower airways of dogs. *J. Appl. Physiol.* **73**, 2305–2313 (1992).
 65. Lai, C. J. & Kou, Y. R. Stimulation of pulmonary rapidly adapting receptors by inhaled wood smoke in rats. *J. Physiol. (Lond.)* **508 (Pt 2)**, 597–607 (1998).
 66. Mills, J. E., Sellick, H. & Widdicombe, J. G. Activity of lung irritant receptors in pulmonary microembolism, anaphylaxis and drug-induced bronchoconstrictions. *J. Physiol. (Lond.)* **203**, 337–357 (1969).
 67. Sellick, H. & Widdicombe, J. G. Stimulation of lung irritant receptors by cigarette smoke, carbon dust, and histamine aerosol. *J. Appl. Physiol.* **31**, 15–19 (1971).
 68. Yu, J. Spectrum of myelinated pulmonary afferents. *AJP: Regulatory, Integrative and Comparative Physiology* **279**, R2142–8 (2000).
 69. Nonomura, K. *et al.* Piezo2 senses airway stretch and mediates lung inflation-induced apnoea. *Nature* **541**, 176–181 (2017).
 70. Matsumoto, S. Effects of vagal stimulation on slowly adapting pulmonary stretch receptors and lung mechanics in anesthetized rabbits. *Lung* **174**, 333–344 (1996).
 71. Krauhs, J. M. Morphology of presumptive slowly adapting receptors in dog trachea. *Anat. Rec.* **210**, 73–85 (1984).
 72. Yamamoto, Y., Atoji, Y. & Suzuki, Y. Calretinin immunoreactive nerve endings in the trachea and bronchi of the rat. *J. Vet. Med. Sci.* **61**, 267–269 (1999).
 73. Schelegle, E. S. & Green, J. F. An overview of the anatomy and physiology of slowly adapting pulmonary stretch receptors. *Respiration Physiology* **125**, 17–31 (2001).
 74. Sampson, S. R. & Vidruk, E. H. Properties of 'irritant' receptors in canine lung. *Respiration Physiology* **25**, 9–22 (1975).
 75. Armstrong, D. J. & LUCK, J. C. A comparative study of irritant and type J receptors in the cat. *Respiration Physiology* **21**, 47–60 (1974).
 76. Kappagoda, C. T., Skepper, J. N., McNaughton, L., Siew, E. E. & Navaratnam, V. Morphology of presumptive rapidly adapting receptors in the rat bronchus. *J. Anat.* **168**, 265–276 (1990).
 77. Chang, R. B., Stochlic, D. E., Williams, E. K., Umans, B. D. & Liberles, S. D. Vagal Sensory Neuron Subtypes that Differentially Control Breathing. *Cell* **161**, 622–633 (2015).
 78. Adriaensen, D. *et al.* Pulmonary intraepithelial vagal nodose afferent nerve terminals are confined to neuroepithelial bodies: an anterograde tracing and

- confocal microscopy study in adult rats. *Cell Tissue Res* **293**, 395–405 (1998).
79. Tansey, E. M. Henry Dale and the discovery of acetylcholine. *Comptes Rendus Biologies* **329**, 419–425 (2006).
 80. Heyman, J. F. & Heyman, C. Recherches physiologiques et pharmacodynamiques sur la tete isolee du chien. *Travail De LInstitut de Pharmacodynamie et de Therapie de LUniversite de Gand* **32**, 1–33 (1926).
 81. Heymans, C. Reflexogenic Areas of the Cardiovascular System. *Perspectives in Biology and Medicine* **3**, 409–417 (1960).
 82. Nowak, S. J. CHRONIC HYPERTENSION PRODUCED BY CAROTID SINUS AND AORTIC-DEPRESSOR NERVE SECTION. *Ann. Surg.* **111**, 102–111 (1940).
 83. Juraschek, S. P. *et al.* Association of History of Dizziness and Long-term Adverse Outcomes With Early vs Later Orthostatic Hypotension Assessment Times in Middle-aged Adults. *JAMA Intern Med* **177**, 1316–9 (2017).
 84. Bainbridge, F. A. The influence of venous filling upon the rate of the heart. *J. Physiol. (Lond.)* **50**, 65–84 (1915).
 85. Paintal, A. S. A STUDY OF VENTRICULAR PRESSURE RECEPTORS AND THEIR ROLE IN THE BEZOLD REFLEX. *Quarterly Journal of Experimental Physiology and Cognate Medical Sciences* **40**, 348–363 (1955).
 86. DAWES, G. S. & Widdicombe, J. G. The afferent pathway of the Bezold reflex: the left vagal branches in dogs. *Br J Pharmacol Chemother* **8**, 395–398 (1953).
 87. Campagna, J. A. & Carter, C. Clinical relevance of the Bezold-Jarisch reflex. *Anesthesiology* **98**, 1250–1260 (2003).
 88. Bronk, D. W. & Stella, G. Afferent Impulses in the Carotid Sinus Nerve: The relation of the discharge from single end organs to arterial blood pressure. *The Journal of Cellular and Comparative Physiology* **1**, 113–130 (1932).
 89. COLERIDGE, H. M. & COLERIDGE, J. C. Cardiovascular afferents involved in regulation of peripheral vessels. *Annu. Rev. Physiol.* **42**, 413–427 (1980).
 90. COLERIDGE, H. M., COLERIDGE, J. C. & Schultz, H. D. Characteristics of C fibre baroreceptors in the carotid sinus of dogs. *J. Physiol. (Lond.)* **394**, 291–313 (1987).
 91. COLERIDGE, H. M. *et al.* Impulses in Slowly Conducting Vagal Fibers from Afferent Endings in the Veins, Atria, and Arteries of Dogs and Cats. *Circulation Research* **33**, 87–97 (1973).
 92. COLERIDGE, H. M., COLERIDGE, J. C., Poore, E. R., Roberts, A. M. & Schultz, H. D. Aortic wall properties and baroreceptor behaviour at normal arterial pressure and in acute hypertensive resetting in dogs. *J. Physiol. (Lond.)* **350**, 309–326 (1984).
 93. COLERIDGE, H. M., COLERIDGE, J. C., Kaufman, M. P. & DANGEL, A. Operational sensitivity and acute resetting of aortic baroreceptors in dogs. *Circulation Research* **48**, 676–684 (1981).
 94. COLERIDGE, J. C., HEMINGWAY, A., HOLMES, R. L. & LINDEN, R. J. The location of atrial receptors in the dog: a physiological and histological study. *J. Physiol. (Lond.)* **136**, 174–197 (1957).
 95. Paintal, A. S. A study of right and left atrial receptors. *J. Physiol. (Lond.)* **120**, 596–610 (1953).
 96. COLERIDGE, H. M., COLERIDGE, J. C. & KIDD, C. CARDIAC RECEPTORS IN THE DOG, WITH PARTICULAR REFERENCE TO TWO TYPES OF AFFERENT ENDING IN THE VENTRICULAR WALL. *J. Physiol. (Lond.)* **174**, 323–339 (1964).

97. Thorén, P. N. Characteristics of left ventricular receptors with nonmedullated vagal afferents in cats. *Circulation Research* **40**, 415–421 (1977).
98. Armour, J. A. Myocardial ischaemia and the cardiac nervous system. *Cardiovasc. Res.* **41**, 41–54 (1999).
99. Kaufman, M. P., Baker, D. G., COLERIDGE, H. M. & COLERIDGE, J. C. Stimulation by bradykinin of afferent vagal C-fibers with chemosensitive endings in the heart and aorta of the dog. *Circulation Research* **46**, 476–484 (1980).
100. Benson, C. J., Eckert, S. P. & McCleskey, E. W. Acid-evoked currents in cardiac sensory neurons: A possible mediator of myocardial ischemic sensation. *Circulation Research* **84**, 921–928 (1999).
101. Thames, M. D. & Minisi, A. J. Reflex responses to myocardial ischemia and reperfusion. Role of prostaglandins. *Circulation* **80**, 1878–1885 (1989).
102. Ustinova, E. E. & Schultz, H. D. Activation of cardiac vagal afferents in ischemia and reperfusion. Prostaglandins versus oxygen-derived free radicals. *Circulation Research* **74**, 904–911 (1994).
103. Sullivan, M. J. *et al.* Non Voltage-Gated Ca²⁺ Influx Through Mechanosensitive Ion Channels in Aortic Baroreceptor Neurons. *Circulation Research* **80**, 861–867 (1997).
104. Lau, O.-C. *et al.* TRPC5 channels participate in pressure-sensing in aortic baroreceptors. *Nature Communications* **7**, 1–12 (2016).
105. Cheng, Z., Powley, T. L., Schwaber, J. S. & Doyle, F. J. A laser confocal microscopic study of vagal afferent innervation of rat aortic arch: chemoreceptors as well as baroreceptors. *J. Auton. Nerv. Syst.* **67**, 1–14 (1997).
106. MILLER, M. R. & KASAHARA, M. STUDIES ON THE NERVE ENDINGS IN THE HEART. *Am. J. Anat.* **115**, 217–233 (1964).
107. Cheng, Z., Powley, T. L., Schwaber, J. S. & Doyle, F. J. Vagal afferent innervation of the atria of the rat heart reconstructed with confocal microscopy. *J. Comp. Neurol.* **381**, 1–17 (1997).
108. Krauhs, J. M. Structure of rat aortic baroreceptors and their relationship to connective tissue. *J. Neurocytol.* **8**, 401–414 (1979).
109. Chalfie, M. Neurosensory mechanotransduction. *Nat Rev Mol Cell Biol* **10**, 44–52 (2009).
110. Coste, B. *et al.* Piezo1 and Piezo2 Are Essential Components of Distinct Mechanically Activated Cation Channels. *Science* **330**, 55–60 (2010).
111. Coste, B. *et al.* Piezo proteins are pore-forming subunits of mechanically activated channels. *Nature* **483**, 176–181 (2013).
112. Kim, S. E., Coste, B., Chadha, A., Cook, B. & Patapoutian, A. The role of Drosophila Piezo in mechanical nociception. *Nature* **483**, 209–212 (2013).
113. Ranade, S. S. *et al.* Piezo2 is the major transducer of mechanical forces for touch sensation in mice. *Nature* **516**, 121–125 (2015).
114. Woo, S.-H. *et al.* Piezo2 is the principal mechanotransduction channel for proprioception. *Nat Neurosci* **18**, 1756–1762 (2015).
115. Woo, S.-H. *et al.* Piezo2 is required for Merkel-cell mechanotransduction. *Nature* **509**, 622–626 (2015).
116. Coste, B. *et al.* Gain-of-function mutations in the mechanically activated ion channel PIEZO2 cause a subtype of Distal Arthrogyrosis. *Proceedings of the National*

- Academy of Sciences* **110**, 4667–4672 (2013).
117. Chesler, A. T. *et al.* The Role of PIEZO2 in Human Mechanosensation. *N. Engl. J. Med.* **375**, 1355–1364 (2016).